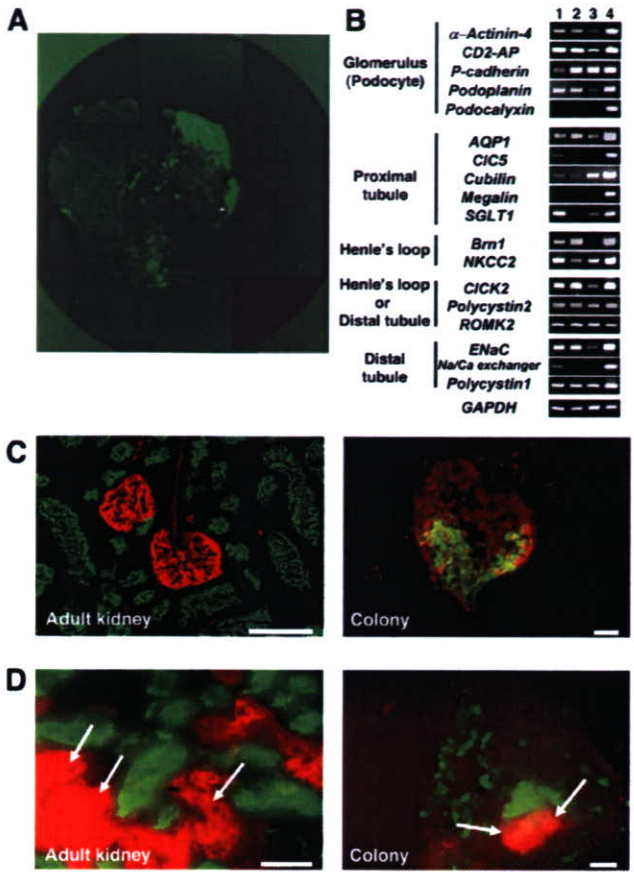

Fig. 2. Colonies are derived from a single multipotent renal progenitor. (**A**) One colony derived from a single cell of EGFP transgenic mesenchyme at culture day 20. (**B**) RT-PCR of three independent wells containing a single cell-derived colony after 20-day culture. Lanes 1-3: colonies; 4: organ culture of E11.5 mesenchyme rudiments. (**C**) Lectin staining of 8-week-old adult kidney (left panel) and a single cell-derived colony (right) with PNA (red, podocyte marker) and with LTL (green, proximal tubule marker). (**D**) Staining of adult kidney (left panel) and a single cell-derived colony (right) with E-cadherin (red, arrow, distal tubule marker) and with LTL (green). Scale bars: 50 μm.

Sall1-GFP^{low} and Sall1-GFP^{negative} (Fig. 3C), and cells in these subpopulations were separated by flow cytometry sorting to be characterized using RT-PCR. As shown in Fig. 3D, Sall1-GFP^{high} cells expressed *Sall1* and *Pax2*. Sall1-GFP^{low} cells expressed markers of stroma (*Foxd1*, previously known as *BF2*), endothelia (*Flk1* and VE-cadherin), and blood cell (*Cd45*), in addition to *Sall1* and *Pax2*. Sall1-GFP^{negative} cells expressed *Flk1* and *Cd45*. The markers of fully differentiated renal epithelia were not expressed in these three populations. These data suggested that cells of stromal lineage were included in cell populations weakly expressing *Sall1* and that those of hemangiogenic lineage were included in both Sall1-GFP^{low} and Sall1-GFP^{negative} populations. Then, the numbers of the colony-forming progenitors in each subpopulation were examined using the low-density culture on 3T3Wnt4 (Fig. 3E). At E11.5, colonies were formed exclusively from the Sall1-GFP^{high} population, and not from Sall1-GFP^{low} or Sall1-GFP^{negative} populations. At E14.5 and 17.5, colonies were also formed only from Sall1-GFP^{high} subpopulations, but the frequency of colony-forming progenitors decreased as gestation proceeded. These results indicate that renal progenitors with multipotent differentiating capacity are included in cell populations strongly expressing *Sall1* throughout gestation periods.

Sall1-GFP^{high} mesenchyme reconstitutes a three-dimensional structure in organ culture

We next examined the in vitro differentiation capacity of three subpopulations in E11.5 mesenchyme by modifying organ culture of mesenchyme rudiments (Grobstein, 1953; Kispert et al., 1998). Sall1-GFP^{high}, Sall1-GFP^{low} and Sall1-GFP^{negative} cells were separated by flow cytometry, aggregated to form a cell pellet by centrifugation and cultured on 3T3Wnt4 feeder cells in an organ culture setting. Starting from day 3 in culture, tubulogenesis was observed only in the aggregate of the Sall1-GFP^{high} population (Fig. 4A, upper panels), while that from Sall1-GFP^{low} or Sall1-GFP^{negative} did not differentiate and disappeared by day 7 (Fig. 4A, lower panels; data of Sall1-GFP^{negative}, not shown). In sections of the Sall1-GFP^{high} aggregate (Fig. 4B), many tubule- (t) and glomerulus-like structures (g) were observed, and the expression of markers for glomerular podocyte (Wt1, Fig. 1C, red) and proximal tubule (LTL, green) was confirmed by confocal microscopy. These data suggest that only Sall1-GFP^{high} cells differentiate into renal epithelia in vitro in a three-dimensional setting, in addition to forming colonies.

Colony size is affected by the absence of *Sall1*

To investigate the role of *Sall1* in colony formation, mesenchymal cells from *Sall1*$^{+/+}$, *Sall1*$^{+/-}$ and *Sall1*$^{-/-}$ embryos at E11.5, which were obtained from intercrosses of *Sall1-GFP* mice, were plated on 3T3Wnt4 feeder cells at a low density. Ten days after culture, double immunostaining using anti-GFP and anti-E-cadherin antibodies was done to strengthen the green fluorescence and to examine the expression of E-cadherin, respectively (Fig. 5). The numbers of colonies formed were not significantly different among wild-type, heterozygous and homozygous mesenchyme, suggesting that colony-forming progenitors do exist and are not decreased in the absence of *Sall1* (data not shown). Colonies derived from *Sall1*$^{+/+}$ wild-type mesenchyme were not stained with GFP (Fig. 5A), while *Sall1*$^{+/-}$ and *Sall1*$^{-/-}$ colonies were positive for GFP (Fig. 5C,E, green), indicating that *Sall1* itself is not required for *Sall1* promoter activity. Colonies from all three groups (*Sall1*$^{+/+}$, *Sall1*$^{+/-}$ and *Sall1*$^{-/-}$) were also positive for E-cadherin (Fig. 5B,D,F), suggesting that differentiation (mesenchymal-to-epithelial transformation) may not be impaired in the absence of *Sall1*. Indeed, marker gene expression for terminally differentiated epithelia in glomeruli and renal tubules was not changed among *Sall1*$^{+/+}$, *Sall1*$^{+/-}$ and *Sall1*$^{-/-}$ colonies on RT-PCR analyses (data not shown). By contrast, the size of *Sall1*$^{-/-}$ colonies (Fig. 5E,F) was significantly smaller than *Sall1*$^{+/+}$ and *Sall1*$^{+/-}$ colonies (Fig. 5B-D), and this was confirmed statistically (Table 1). Thus, *Sall1* is not

Table 1. Colonies derived from *Sall1*-mutant metanephric mesenchyme

Genotype	Embryos*	Area at day 10 (mean±s.d.) (μm^2) (n=60)	P
+/+	2	16,118±7219	
+/–	2	16,318±7473	0.44
–/–	2	5140±2071	<0.001

*Number of embryos examined. P values were analyzed against wild type (+/+) using a t-test. Embryos of a total of four litters were analyzed in this way. Representative data from one experiment are shown.

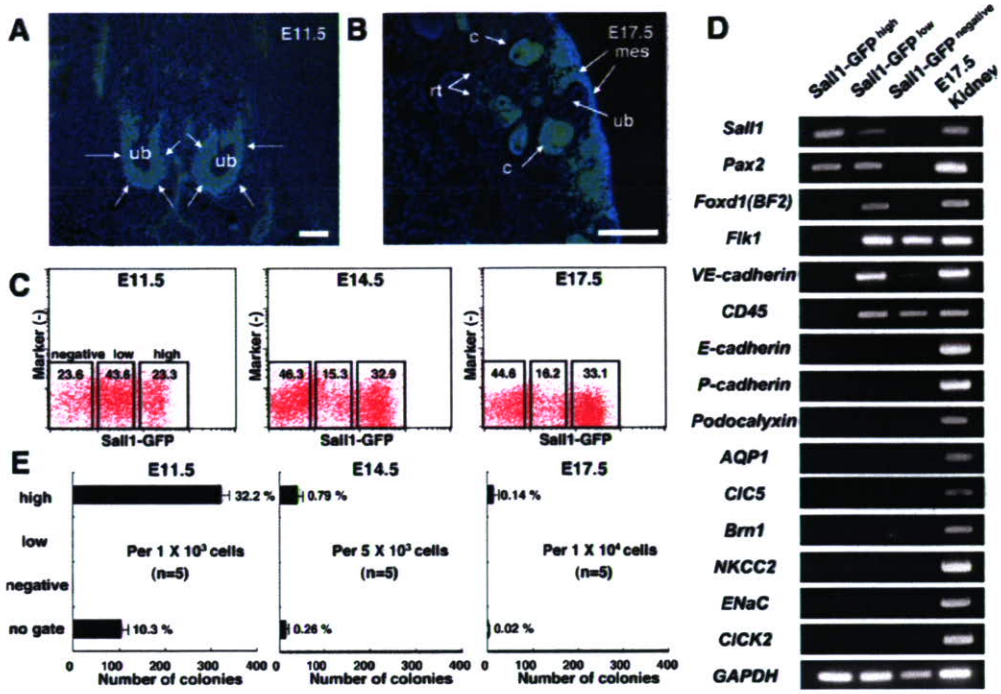

Fig. 3. Colony-forming progenitors exist in the Sall1-GFP^{high} subpopulation of the metanephros. (**A**,**B**) Cryosections of metanephros of *Sall1-GFP* knock-in mouse (A: E11.5; B: E17.5). Blue: DAPI. (**C**) Metanephros contains three subpopulations (Sall1-GFP^{high}, Sall1-GFP^{low} and Sall1-GFP^{negative}). The percentages of the subpopulations at each fetal stage are shown. Figures are the average of five independent experiments. (**D**) RT-PCR analysis of three subpopulations included in E11.5 mesenchyme. (**E**) Numbers of colonies in each subpopulation derived from E11.5 mesenchyme, E14.5 and E17.5 metanephros. The numbers of colony were counted after 20-day culture. The graph shows the average of five independent experiments. ub, ureteric bud; mes, mesenchyme; c, C-shaped body; rt, renal tubule. Scale bars: 50 μm.

required for generation or differentiation of renal progenitors, but the colony size is affected by *Sall1* absence. This is consistent with our previous report that *Sall1*-deficient mesenchyme is competent with respect to epithelial differentiation tested by spinal cord recombination (Nishinakamura et al., 2001). In the spinal cord recombination experiments, *Sall1*-deficient mesenchyme was consistently smaller than wild-type mesenchyme, but this could be due to differences in the initial size of the mesenchyme. Using the colony-forming assay starting from a single cell, we now show that *Sall1* is indeed required for the colony from the mesenchyme to develop into a normal size.

The PCP pathway regulates colony size and the differentiation of colony-forming cells

By combining the colony-forming assay set up in this study and gene transfer using retroviral vector *pMY-IRES-EGFP* (Morita et al., 2000; Kitamura et al., 2003), we observed EGFP expression in 12.9% of colony-forming progenitor cells (116 colonies expressing green fluorescence per total of 896 colonies formed from three independent experiments). Thus, the colony-forming assay in this study enables us to investigate direct effects of reagents and gene transduction on colony-forming progenitor cells, allowing us to examine the roles of Wnt and its downstream branches in kidney development. Positive immunostaining of the colonies for activated JNK1 and 2 indicated that the JNK branch of the PCP pathways (Boutros et al., 1998) may be activated downstream of Wnt4 (Fig. 6A). Indeed, the addition of two kinds of JNK inhibitor (JNKI1 and JNKI2) (Bonny et al., 2001; Bennett et al., 2001) gave rise to smaller colonies than did the control without reagents (Fig. 6B,C, colonies from EGFP transgenic mesenchyme, Table 2). The result of control experiments using the HIV-TAT peptide excluded the possibility that the effects of JNKI1 were derived from non-specific toxicity of the peptide constituting the inhibitor (Fig. 6B). We then investigated effects of both activation and inactivation of Rac1, one of the Rho family GTPases implicated in PCP pathways (Habas et al., 2003), on colony formation. Cells from wild-type E11.5 mesenchyme were transduced with both constitutively active (CA) and dominant-negative (DN) forms of *Rac1* using the retroviral vector *pMY-IRES-EGFP*. Colonies consisting of cells expressing both EGFP and CA-Rac1 were larger than those transduced with *pMY-IRES-EGFP* controls (Fig. 6D, Table 3), suggesting positive effects on colony size. By contrast, the transduction of DN-*Rac1* gave rise to smaller

Table 2. Effects of reagents on the area of colony

Reagent	*n*	Area at day 10 (mean±s.d.) (μm²)	*P*
Control (without reagents)	20	35,429±15,132	
HIV-TAT peptide	20	38,198±11,357	0.25
JNK inhibitor 1	20	7771±4520	<0.001
Control (without reagents)	30	36,330±15,065	
JNK inhibitor 2	20	6687±2834	<0.001
Y27,632	20	92,359±24,768	<0.001
LiCl	20	5687±3535	<0.001
BIO	30	7436±4897	<0.001
Dkk-1	20	31,998±12,566	0.147

n, number of colonies measured. *P* values were analyzed against control using a *t*-test. For each reagent, more than three independent experiments were performed. Representative data from one experiment are shown.

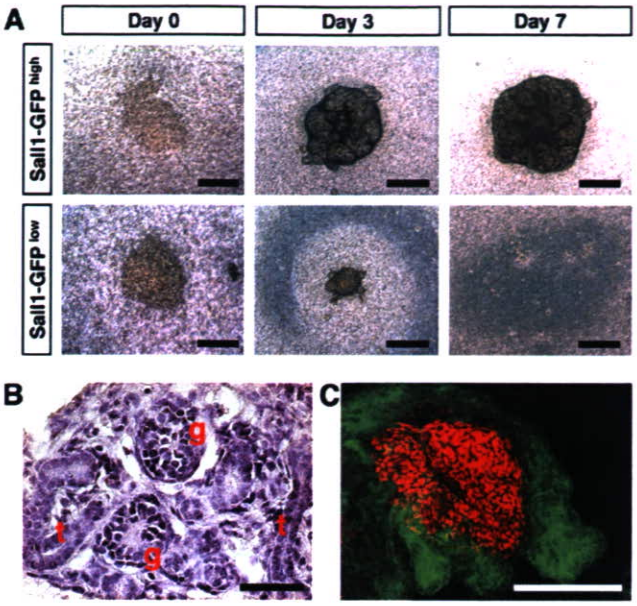

Fig. 4. Sall1-GFP^{high} mesenchyme differentiates into renal epithelia in organ culture. (**A**) Three subpopulations in E11.5 mesenchyme (Sall1-GFP^{high}, Sall1-GFP^{low} and Sall1-GFP^{negative}) were cultured on 3T3Wnt4 feeder cells in an organ culture setting. Only Sall1-GFP^{high} cells (upper panels) differentiated into kidney structure, while Sall1-GFP^{low} cells (lower) disappeared. (**B**) Hematoxylin-eosin staining of sections of Sall1-GFP^{high} aggregates at day 10. Tubule- and glomerulus-like structures are seen. (**C**) Double staining with Wt1 (red, podocyte marker) and LTL (green, proximal tubule marker) of Sall1-GFP^{high} aggregates. g, glomerulus-like structure; t, tubule-like structure. Scale bars: 500 μm in A; 25 μm in B,C.

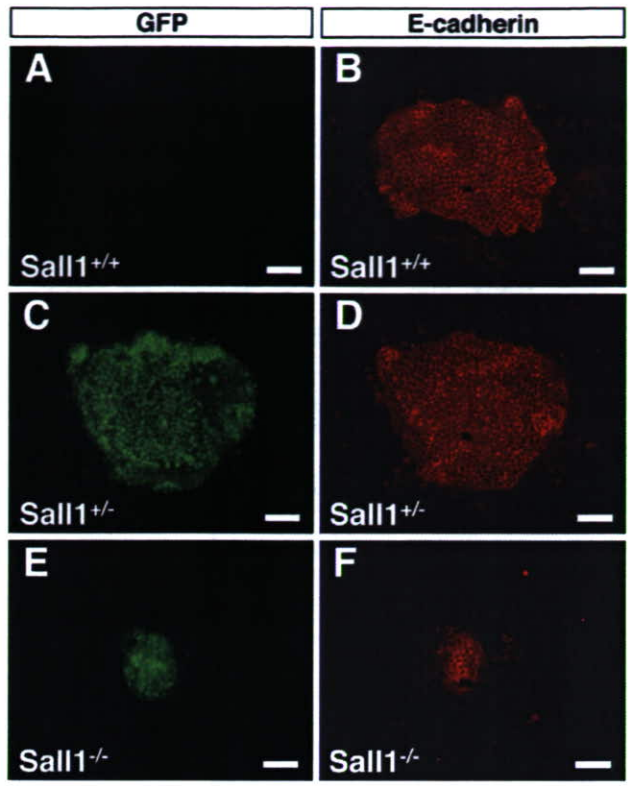

Fig. 5. Colony formation from *Sall1*-mutant metanephric mesenchyme obtained from intercrosses of *Sall1-GFP* mice. (**A-F**) Colonies derived from *Sall1*$^{+/+}$ (A,B), *Sall1*$^{+/-}$ (C,D) and *Sall1*$^{-/-}$ (E,F) mesenchyme were stained both with anti-GFP (A,C,E, green) and with anti-E-cadherin antibodies (B,D,F, red). *Sall1*-deficient colonies (E,F) were significantly smaller than those from wild-type (A,B) and heterozygous (C,D) mesenchyme. Scale bars: 50 μm.

colonies than did the controls (Fig. 6D, Table 3). The numbers of colonies formed were not significantly changed either with the addition of inhibitors or with gene transduction (data not shown). These data indicate that Rac and JNK pathways positively regulate colony size.

By contrast, inactivation of the Rho/Rho-associated protein kinase (ROCK) pathway, another branch of PCP (Strutt et al., 1997; Winter et al., 2001; Habas et al., 2001; Habas et al., 2003), with the addition of ROCK inhibitor, Y27,632 (Uehata et al., 1997) (Fig. 6E, colonies from EGFP transgenic mesenchyme, Table 2), or the transduction of DN-*RhoA*, increased the colony size (Fig. 6F, Table 3), while the activation with CA-*RhoA* decreased it (Fig. 6F, Table 3). Activation of β-catenin signaling both with the addition of two kinds of glycogen synthetase kinase (GSK)-3 inhibitors, lithium chloride (LiCl) (Klein and Melton, 1996) (Fig. 6G, colonies from EGFP transgenic mesenchyme, Table 2) and (2′Z, 3′E)-6-Bromoindirubin-3′-oxime (BIO) (Sato et al., 2004) (Table 2) and with the transduction of the active form of *β-catenin* (Fig. 6H, Table 3) gave rise to smaller colonies. However, inactivation of the β-catenin pathway with the addition of recombinant dickkopf homolog 1 (Dkk-1), a specific inhibitor of the β-catenin pathway (Glinka et al., 1998) and with the transduction of axin (Zeng et al., 1997) exerted no significant effects on colony formation (Tables 2, 3). These data suggest inhibitory roles of Rho/ROCK and β-catenin pathways in regulating colony size.

Table 3. Effects of gene transduction on the area of colony

Gene transduced	*n*	Area at day 20 (mean±s.d.) (μm²)	*P*
Control (vector)	23	49,666±32,111	
CA-*Rac1*	12	83,990±52,619	0.01
DN-*Rac1*	24	23,045±22,791	<0.001
CA-*RhoA*	12	25,658±19,205	<0.005
DN-*RhoA*	21	89,723±49,989	0.001
Control (vector)	38	62,013±31,212	
Active-*β-catenin*	20	23,241±21,685	<0.001
Axin	22	65,352±27,675	0.34

n, number of colonies measured. *P* values were analyzed against control using a *t*-test. Data from three independent experiments is shown.

RT-PCR analysis showed that the expression of marker genes (E-cadherin, P-cadherin, podocalyxin, *Aqp1, Clc5, Brn1, Nkcc2, ENaC* and *Clck2*) was inhibited with the addition of JNK inhibitors (Fig. 6I). Although the addition of LiCl and JNK inhibitors resulted in a decreased size of colonies to the same extent, immunostaining confirmed that E-cadherin was lost with JNK inhibitors 1 and 2, but not with LiCl (Fig. 6J, colonies from EGFP transgenic mesenchyme). Thus, the JNK pathway is likely not only to regulate colony size but also to be involved in epithelialization (mesenchymal-to-epithelial transformation) of colony-forming progenitors.

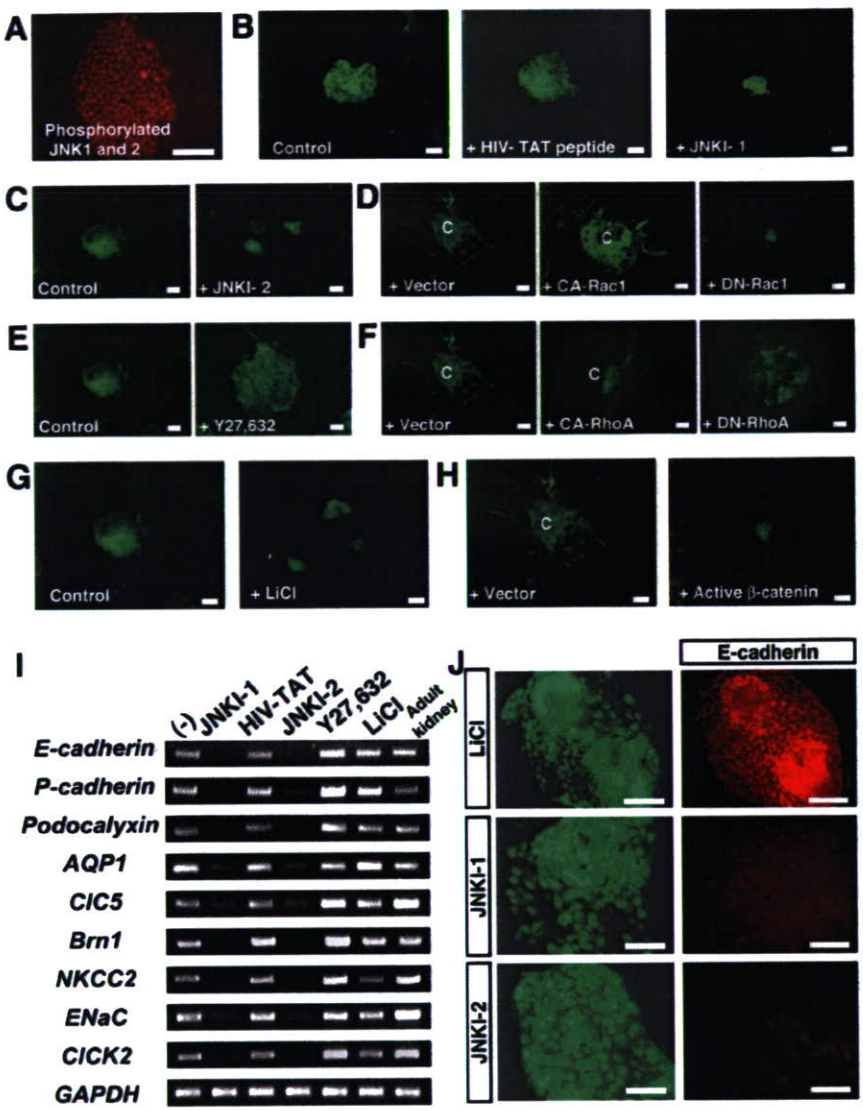

Fig. 6. PCP pathways regulate colony size and the differentiation of colony-forming cells. (**A**) Immunostaining of activated JNK1 and 2 in the colony. (**B**,**C**) The addition of two kinds of JNK inhibitors (JNKI1 and JNKI2, 10 μmol/l) gave rise to smaller colonies than did the control without reagents or HIV-TAT peptide (10 μmol/l). (**D**) The transduction of CA-*Rac1* resulted in an increase in colony size, whereas that of DN-*Rac1* resulted in a decrease. (**E**,**F**) The addition of Y27,632 (E, 10 μmol/l), or the transduction of DN-*RhoA*, increased colony size, while activation with CA-*RhoA* decreased it (F). (**G**,**H**) Activation of the β-catenin pathway by adding LiCl (G, 10 μmol/l) or transducing the active form of *β-catenin* (H) gave rise to smaller colonies. (**I**) RT-PCR analysis of colonies treated with JNKI-1, HIV-TAT peptide, JNKI-2, Y27,632 and LiCl. (**J**) E-cadherin expression was lost with JNKI-1 and -2 but not with LiCl. EGFP transgenic mesenchyme was used for B,C,E,G and J, while wild type was used for D,F and H, to visualize colonies infected by retrovirus vectors. c, colony. Scale bars: 50 μm.

The PCP pathway is involved in tubulogenesis in organ culture

To examine if the results described above were consistent with kidney formation in vivo, we tested the effect of the reagents on whole metanephroi (Fig. 7A-E) and mesenchyme rudiments (F-J) in an organ culture setting. After 7 days of culture, the size of kidney structures was measured. As compared with the control explants cultured without reagents (Fig. 7A,F), the addition of JNK inhibitor 1 (Fig. 7B,G) and JNK inhibitor 2 (Fig. 7C,H) and LiCl (Fig. 7E,J) resulted in a decrease in the size of kidney structures developed, while the addition of ROCK inhibitor Y27,632 (Fig. 7D,I) gave rise to larger ones. These findings were observed both in whole kidney and in mesenchyme rudiments, and were confirmed statistically (Table 4). We also evaluated the effect of the reagents on tubule formation and branching of ureteric bud by staining with an antibody against secreted frizzled-related

Table 4. Effects of reagents on the area of organ culture

	Whole metanephroi			Mesenchymal rudiments		
Reagent	*n*	Area at day 7 (mean ± s.d.) (mm²)	*P*	*n*	Area at day 7 (mean ± s.d.) (mm²)	*P*
Control (without reagents)	7	1.717±0.381		6	1.912±0.200	
HIV-TAT peptide	5	1.500±0.215	0.12	7	1.838±0.364	0.33
JNK inhibitor 1	6	1.020±0.325	<0.005	7	0.651±0.131	<0.001
JNK inhibitor 2	6	1.105±0.260	<0.005	7	1.078±0.377	<0.001
Y27,632	5	2.871±0.879	<0.01	7	3.401±0.433	<0.001
LiCl	5	0.716±0.070	<0.001	7	1.270±0.238	<0.001

n, number of explants measured. *P* values were analyzed against control by using a *t*-test. Data from five independent experiments each for whole metanephroi and mesenchyme rudiments are shown.

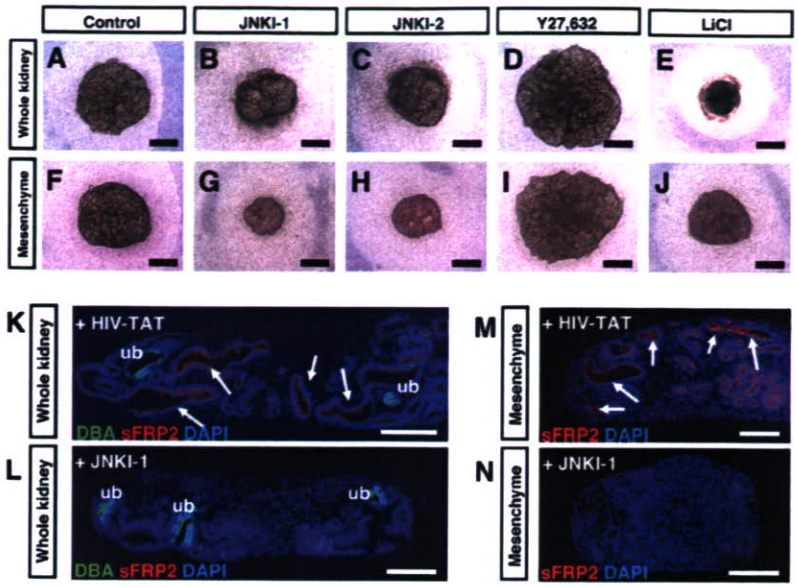

Fig. 7. Effects of reagents on tubulogenesis in organ culture. Whole metanephroi (**A-E**) and mesenchyme rudiments (**F-J**) cultured for 7 days. (A,F) Control explants without reagents, (B,G) 10 μmol/l JNK inhibitor 1 (JNKI1), (C,H) 10 μmol/l JNKI2, (D,I) 10 μmol/l Y27,632, (E,J) 20 mmol/l (E) and 10 mmol/l (J) LiCl. (**K,L**) Section staining using DBA (green), an anti-sFRP2 antibody (red) and DAPI (blue) on whole kidneys treated with 15 μmol/l HIV-TAT peptide (K) and JNKI-1 (L). (**M,N**) Double labeling with sFRP2 and DAPI on mesenchyme rudiments treated with HIV-TAT peptide (M) and JNKI-1 (N). ub, ureteric bud. Scale bars: 500 μm in A-J; 200 μm in K-N.

protein 2 (sFRP2; Fig. 7K-N, red), the gene expressed only in newly formed tubular epithelia (Lescher et al., 1998), and DBA (Fig. 7K,L, green), respectively. While some tubules expressing sFRP2 were found in explants treated with control HIV-TAT peptide (Fig. 7K,M, arrows), they were lost with JNK inhibitor 1 both in whole metanephroi (Fig. 7L) and in mesenchyme explants (Fig. 7N), suggesting the involvement of JNK pathways in mesenchymal-to-epithelial transformation in organ culture. By contrast, branching of ureteric bud was proportional to the size of explants, and there were no specific effects of the reagents observed on the ureteric bud itself (data not shown). These findings were consistent with the results observed in the colony-forming assay (Fig. 6, Table 2). Thus our colony-forming assay, which enables analysis at a single cell level, could be used for examining mechanisms of three-dimensional kidney development.

DISCUSSION

Renal progenitors defined by colony-forming assay

In this study, we provide evidence, using in vitro clonal analysis combined with flow cytometry, for the presence of progenitor cells in the fetal mouse kidney. Results of staining with PNA, LTL and E-cadherin, and of RT-PCR showed the differentiating capacity of a single Sall1-GFP^{high} cell into glomerular epithelia (podocyte), proximal and distal tubule, respectively. In addition to lineage-marker expression, both glomerulus- and tubule-like structures were reconstituted by Sall1-GFP^{high} cells, supporting their differentiation ability. A multipotent renal stem cell line has been isolated from E11.5 mesenchyme utilizing immortalization with T antigen of SV40 virus (Oliver et al., 2002). The cell line expresses marker genes of endothelia and smooth muscle cells with treatment of TGFβ1, in addition to gene expression of mesenchyme and renal epithelia. It has not been known, however, whether they normally resided in the fetal kidney or accidentally emerged by the influence of the process with immortalization. In our colony-forming system, gene expression of endothelia and smooth muscle cells was not observed, and expression of *Foxd1* (*BF2*), a marker gene specific to stroma, a third cell population included in metanephros was not found (data not shown). Thus, it remains to be elucidated whether embryonic kidney contains stem cells that can differentiate into endothelium, smooth muscle or stroma in addition to epithelia of glomerulus and renal tubules.

The renal progenitors defined by our colony-forming assay are included in cell populations strongly expressing *Sall1* throughout gestation periods, and they might continue to reside in the outer layer of embryonic kidney, where undifferentiated metanephric mesenchyme resides and strongly expresses *Sall1* (Fig. 3B). As shown in Table 5, the total cell numbers of metanephros increased and the frequency of colony-forming Sall1-GFP^{high} cells decreased as gestation proceeded. Interestingly, the calculated numbers of the colony-forming cells remained almost constant throughout gestation periods (400-800 cells/embryonic kidney). The amplification of these progenitors might not occur in the embryonic kidney. One interesting question is whether they continue to remain in the adult kidney. From 8-week-old mice, however, colonies were not formed under the same culture conditions (data not shown). Renal progenitors defined by our colony-forming assay might be lost by the time kidney development is complete.

Table 5. Calculated number of colony-forming progenitors in embryonic kidney

	E11.5	E14.5	E17.5
Total cell number of kidney ($\times 10^4$)	0.77±0.24	21.4±2.7	77.9±19.4
Sall1-GFP^{high} cells in kidney (%)	23.6±1.7	46.3±2.1	44.5±0.9
Colony formation in Sall1-GFP^{high} cells (%)	32.2±2.8	0.79±0.18	0.14±0.07
Calculated numbers of colony-forming cells*	585.1	782.7	485.3

Mean±s.d. (from five independent experiments each for E11.5, E14.5, and E17.5).
*Numbers of colony-forming cells were calculated by multiplying the means of the three values above.

Analysis of gene function in kidney development by colony-forming assay

The knowledge of gene function in kidney development has mainly been obtained from analyses using knockout mice, while experimental systems that investigate gene function in individual cells of metanephros have been lacking. By setting up a novel system combining colony formation from a single cell and gene transduction using a retroviral vector, our culture system enables the direct observation of effects of reagents and gene transduction on colony-forming progenitor cells. As similar results were obtained from organ culture experiments (Fig. 7), it is less likely that the cellular behavior observed in our colony-assay system might be artifactual.

Mice lacking the constituent genes involved in downstream branches of Wnt signaling pathways often show early embryonic lethality, such as *Rac1* (Sugihara et al., 1998), *Jnk1* and *Jnk2* (Kuan et al., 1999), β-catenin (Haegel et al., 1995), axin (Zeng et al., 1997), and their functions in kidney morphogenesis remain largely unknown. Using our culture system, functions of these genes in metanephros development were elucidated. Furthermore, experiments for colony formation from mesenchyme of *Sall1*-mutant embryos demonstrated the roles of *Sall1* for the colony size. Thus, the colony-assay system set up in this study can also be applied to the analysis of genetic mouse models.

Roles of PCP pathway in kidney development

Among downstream branches of Wnt4 signal, we found that Rac- and JNK-dependent PCP pathways positively regulated the colony size and the differentiation of colony-forming cells. This result is compatible with several previous reports (Du et al., 1995; Ungar et al., 1995; Maretto et al., 2003). In frogs and fish, the Wnt4 family does not strongly activate the β-catenin pathway, and affects convergent extension, which is polarized movement during embryonic development regulated by the PCP pathway (Du et al., 1995; Ungar et al., 1995). Activation of the β-catenin signaling was not detected at various stages of differentiation of the metanephric mesenchyme, which was examined using transgenic mice expressing the *lacZ* reporter genes under the control of β-catenin/TCF responsive elements (Maretto et al., 2003). Furthermore, activation of the β-catenin pathway is implicated in epithelial-to-mesenchymal transition during mesoderm formation in embryonic development and tumorigenesis (Polakis, 2000; Bienz and Clevers, 2000), which is opposite to the process we examined in this study: mesenchymal-to-epithelial transformation. Thus it may be possible that PCP pathways, not the β-catenin pathway, play central roles as downstream branches of Wnt4 for epithelial differentiation of metanephric mesenchyme.

We demonstrated that Rac1 and RhoA play positive and negative roles for the regulation of colony size, respectively. The Rho family of small GTPases is known to be implicated in cell proliferation by the regulation of cell cycle progression, in addition to its effects on the cytoskeleton (Etienne-Manneville and Hall, 2002). Antagonism, or the opposing activities, between two Rho GTPases have been noted in some cell types (Luo, 2000; Gu et al., 2005). For instance, a hematopoietic-specific Rho GTPase, RhoH, negatively regulates both growth and actin-based function of hematopoietic progenitors via suppression of Rac-mediated signaling (Gu et al., 2005). Similarly, our data suggested the possibility that Rac1 and RhoA might antagonistically regulate the growth of progenitors in kidney development. Recently the roles of the JNK pathway in epithelial morphogenesis have been noted both in *Drosophila* and in mice (Xia and Karin, 2004). Our data also suggested the essential roles of JNK pathways in epithelialization, as well as in regulation of colony size. Common mechanisms regulating epithelial morphogenesis might underlie these processes. The PCP pathways, including the Rho family of small GTPases and JNK, control several developmental processes, mainly by regulating cell cytoskeletons, such as the polarity of hairs on the epidermal cells of *Drosophila* wings, the arrangement of ommatidial cells of *Drosophila* eyes, the polarity of stereocilia in the inner ears of mammals, and convergent extension in *Xenopus* and zebrafish (Veeman et al., 2003; Wallingford et al., 2002). In addition to these processes, we provide a novel hypothesis of the involvement of the PCP pathways in kidney development.

In summary, we set up a novel colony-forming assay by which we demonstrated the presence and the frequency of multipotent progenitor cells in embryonic kidneys. This assay would serve as a useful tool for analyzing differentiation mechanisms in the kidney at a single cell level, taking advantage of the facility of gene transfer.

We thank Dr M. Okabe for providing EGFP transgenic mice, Dr A. Kikuchi for *pBSKS-rAxin*, Dr A. Nagafuchi for *pUC-EF-1α-β-catenin^{SA}-3HA*, Dr H. Koide for *pCAGIP-flag-Rac1* and *RhoA*, Dr T. Kitamura for *pMY-IRES-EGFP* and PLAT-E, Y. Morita for technical support for FACS, and Dr C. Kobayashi for critically reading the manuscript. This work was partly supported by the Ministry of Health, Labor, and Welfare of Japan.

References

Barasch, J., Yang, J., Ware, C. B., Taga, T., Yoshida, K., Erdjument-Bromage, H., Tempst, P., Parravicini, E., Malach, S., Aranoff, T. et al. (1999). Mesenchymal to epithelial conversion in rat metanephros is induced by LIF. *Cell* **99**, 377-386.

Bennett, B. L., Sasaki, D. T., Murray, B. W., O'Leary, E. C., Sakata, S. T., Xu, W., Leisten, J. C., Motiwala, A., Pierce, S., Satoh, Y. et al. (2001). SP600125, an anthrapyrazolone inhibitor of Jun N-terminal kinase. *Proc. Natl. Acad. Sci. USA* **98**, 13681-13686.

Bienz, M. and Clevers, H. (2000). Linking colorectal cancer to Wnt signaling. *Cell* **103**, 311-320.

Bonny, C., Oberson, A., Negri, S., Sauser, C. and Schorderet, D. F. (2001). Cell-permeable peptide inhibitors of JNK: novel blockers of beta-cell death. *Diabetes* **50**, 77-82.

Boutros, M., Paricio, N., Strutt, D. I. and Mlodzik, M. (1998). Dishevelled activates JNK and discriminates between JNK pathways in planar polarity and Wingless signaling. *Cell* **94**, 109-118.

Bradley, T. R. and Metcalf, D. (1966). The growth of mouse bone marrow cells in vitro. *Aust. J. Exp. Biol. Med. Sci.* **44**, 287-299.

Carroll, T. J., Park, J. S., Hayashi, S., Majumdar, A. and McMahon, A. P. (2005). Wnt9b plays a central role in the regulation of mesenchymal to epithelial transitions underlying organogenesis of the mammalian urogenital system. *Dev. Cell* **9**, 283-292.

Du, S. J., Purcell, S. M., Christian, J. L., McGrew, L. L. and Moon, R. T. (1995). Identification of distinct classes and functional domains of Wnts through expression of wild-type and chimeric proteins in *Xenopus* embryos. *Mol. Cell. Biol.* **15**, 2625-2634.

Etienne-Manneville, S. and Hall, A. (2002). Rho GTPases in cell biology. *Nature* **420**, 629-635.

Gilbert, T., Gaonach, S., Moreau, E. and Merlet-Benichou, C. (1994). Defect of nephrogenesis induced by gentamicin in rat metanephric organ culture. *Lab. Invest.* **70**, 656-666.

Glinka, A., Wu, W., Delius, H., Monaghan, A. P., Blumenstock, C. and Niehrs, C. (1998). Dickkopf-1 is a member of a new family of secreted proteins and functions in head induction. *Nature* **391**, 357-362.

Grobstein, C. (1953). Inductive epithelio-mesenchymal interaction in cultured organ rudiments of the mouse metanephros. *Science* **118**, 52-55.

Gu, Y., Jasti, A. C., Jansen, M. and Siefring, J. E. (2005). RhoH, a hematopoietic-specific Rho GTPase, regulates proliferation, survival, migration, and engraftment of hematopoietic progenitor cells. *Blood* **105**, 1467-1475.

Habas, R., Kato, Y. and He, X. (2001). Wnt/Frizzled activation of Rho regulates vertebrate gastrulation and requires a novel Formin homology protein Daam1. *Cell* **107**, 843-854.

Habas, R., Dawid, I. B. and He, X. (2003). Coactivation of Rac and Rho by Wnt/Frizzled signaling is required for vertebrate gastrulation. *Genes Dev.* **17**, 295-309.

Haegel, H., Larue, L., Ohsugi, M., Fedorov, L., Herrenknecht, K. and Kemler, R. (1995). Lack of beta-catenin affects mouse development at gastrulation. *Development* **121**, 3529-3537.

Herzlinger, D., Koseki, C., Mikawa, T. and Al-Awqati, Q. (1992). Metanephric mesenchyme contains multipotent stem cells whose fate is restricted after induction. *Development* **114**, 565-572.
Herzlinger, D., Qiao, J., Cohen, D., Ramakrishna, N. and Brown, A. M. C. (1994). Induction of kidney epithelial morphogenesis by cells expressing *Wnt-1*. *Dev. Biol.* **166**, 815-818.
Ikeda, S., Kishida, S., Yamamoto, H., Murai, H., Koyama, S. and Kikuchi, A. (1998). Axin, a negative regulator of the Wnt signaling pathway, forms a complex with GSK-3beta and beta-catenin and promotes GSK-3beta-dependent phosphorylation of beta-catenin. *EMBO J.* **17**, 1371-1384.
Kispert, A., Vainio, S. and McMahon, A. P. (1998). Wnt-4 is a mesenchymal signal for epithelial transformation of metanephric mesenchyme in the developing kidney. *Development* **125**, 4225-4234.
Kitamura, T., Koshino, Y., Shibata, F., Oki, T., Nakajima, H., Nosaka, T. and Kumagai, H. (2003). Retrovirus-mediated gene transfer and expression cloning: powerful tools in functional genomics. *Exp. Hematol.* **31**, 1007-1014.
Klein, P. S. and Melton, D. A. (1996). A molecular mechanism for the effect of lithium on development. *Proc. Natl. Acad. Sci. USA* **93**, 8455-8459.
Kuan, C. Y., Yang, D. D., Samanta Roy, D. R., Davis, R. J., Rakic, P. and Flavell, R. A. (1999). The Jnk1 and Jnk2 protein kinases are required for regional specific apoptosis during early brain development. *Neuron* **22**, 667-676.
Lescher, B., Haenig, B. and Kispert, A. (1998). sFRP-2 is a target of the Wnt-4 signaling pathway in the developing metanephric kidney. *Dev. Dyn.* **213**, 440-451.
Luo, L. (2000). Rho GTPases in neuronal morphogenesis. *Nat. Rev. Neurosci.* **1**, 173-180.
Maretto, S., Cordenonsi, M., Dupont, S., Braghetta, P., Broccoli, V., Hassan, A. B., Volpin, D., Bressan, G. M. and Piccolo, S. (2003). Mapping Wnt/β-catenin signaling during mouse development and in colorectal tumors. *Proc. Natl. Acad. Sci. USA* **100**, 3299-3304.
Miller, J. R., Hocking, A. M., Brown, J. D. and Moon, R. T. (1999). Mechanism and function of signal transduction by the Wnt/β-catenin and Wnt/Ca^{2+} pathways. *Oncogene* **18**, 7860-7872.
Miyagishi, M., Fujii, R., Hatta, M., Yoshida, E., Araya, N., Nagafuchi, A., Ishihara, S., Nakajima, T. and Fukamizu, A. (2000). Regulation of Lef-mediated transcription and p53-dependent pathway by associating beta-catenin with CBP/p300. *J. Biol. Chem.* **275**, 35170-35175.
Morita, S., Kojima, T. and Kitamura, T. (2000). Plat-E: an efficient and stable system for transient packaging of retroviruses. *Gene Ther.* **7**, 1063-1066.
Nishinakamura, R., Matsumoto, Y., Nakao, K., Nakamura, K., Sato, A., Copeland, N. G., Gilbert, D. J., Jenkins, N. A., Scully, S., Lacey, D. L. et al. (2001). Murine homolog of *SALL1* is essential for ureteric bud invasion in kidney development. *Development* **128**, 3105-3115.
Okabe, M., Ikawa, M., Kominami, K., Nakanishi, T. and Nishimune, Y. (1997). 'Green mice' as a source of ubiquitous green cells. *FEBS Lett.* **407**, 313-319.
Oliver, J. A., Barasch, J., Yang, J., Herzlinger, D. and Al-Awqati, Q. (2002). Metanephric mesenchyme contains embryonic renal stem cells. *Am. J. Physiol.* **283**, F799-F809.
Plisov, S. Y., Yoshino, K., Dove, L. F., Higinbotham, K. G., Rubin, J. S. and Perantoni, A. O. (2001). TGFβ2, LIF and FGF2 cooperate to induce nephrogenesis. *Development* **128**, 1045-1057.
Pluznik, D. H. and Sachs, L. (1965). The cloning of normal "mast" cells in tissue culture. *J. Cell Physiol.* **66**, 319-324.
Polakis, P. (2000). Wnt signaling and cancer. *Genes Dev.* **14**, 1837-1851.
Reynolds, B. A., Tetzlaff, W. and Weiss, S. (1992). A multipotent EGF-responsive striatal embryonic progenitor cell produces neurons and astrocytes. *J. Neurosci.* **12**, 4565-4574.
Sato, N., Meijer, L., Skaltsounis, L., Greengard, P. and Brivanlou, A. H. (2004). Maintenance of pluripotency in human and mouse embryonic stem cells through activation of Wnt signaling by a pharmacological GSK-3-specific inhibitor. *Nat. Med.* **10**, 55-63.
Saxen, L. (1987). *Organogenesis of the Kidney*. New York: Cambridge University Press.
Stark, K., Vainio, S., Vassileva, G. and McMahon, A. P. (1994). Epithelial transformation of metanephric mesenchyme in the developing kidney regulated by Wnt-4. *Nature* **372**, 679-683.
Strutt, D. I., Weber, U. and Mlodzik, M. (1997). The role of RhoA in tissue polarity and Frizzled signaling. *Nature* **387**, 292-295.
Sugihara, K., Nakatsuji, N., Nakamura, K., Nakao, K., Hashimoto, R., Otani, H., Sakagami, H., Kondo, H., Nozawa, S., Aiba, A. et al. (1998). Rac1 is required for the formation of three germ layers during gastrulation. *Oncogene* **17**, 3427-3433.
Takasato, M., Osafune, K., Matsumoto, Y., Kataoka, Y., Yoshida, N., Meguro, H., Aburatani, H., Asashima, M. and Nishinakamura, R. (2004). Identification of kidney mesenchymal genes by a combination of microarray analysis and *Sall1-GFP* knockin mice. *Mech. Dev.* **121**, 547-557.
Uehata, M., Ishizaki, T., Satoh, H., Ono, T., Kawahara, T., Morishita, T., Tamakawa, H., Yamagami, K., Inui, J., Maekawa, M. et al. (1997). Calcium sensitization of smooth muscle mediated by a Rho-associated protein kinase in hypertension. *Nature* **389**, 990-994.
Ungar, A. R., Kelly, G. M. and Moon, R. T. (1995). Wnt4 affects morphogenesis when misexpressed in the zebrafish embryo. *Mech. Dev.* **52**, 153-164.
Veeman, M. T., Axelrod, J. D. and Moon, R. T. (2003). A second canon: functions and mechanisms of β-catenin-independent Wnt signaling. *Dev. Cell* **5**, 367-377.
Wallingford, J. B., Fraser, S. E. and Harland, R. M. (2002). Convergent extension: the molecular control of polarized cell movement during embryonic development. *Dev. Cell* **2**, 695-706.
Winter, C. G., Wang, B., Ballew, A., Royou, A., Karess, R., Axelrod, J. D. and Luo, L. (2001). *Drosophila* Rho-associated kinase (Drok) links Frizzled-mediated planar cell polarity signaling to the actin cytoskeleton. *Cell* **105**, 81-91.
Wodarz, A. and Nusse, R. (1998). Mechanisms of Wnt signaling in development. *Annu. Rev. Cell Dev. Biol.* **14**, 59-88.
Xia, Y. and Karin, M. (2004). The control of cell motility and epithelial morphogenesis by Jun kinases. *Trends Cell Biol.* **14**, 94-101.
Zeng, L., Fagotto, F., Zhang, T., Hsu, W., Vasicek, T. J., Perry, W. L., 3rd, Lee, J. J., Tilghman, S. M., Gumbiner, B. M. and Costantini, F. (1997). The mouse Fused locus encodes Axin, an inhibitor of the Wnt signaling pathway that regulates embryonic axis formation. *Cell* **90**, 181-192.

Available online at www.sciencedirect.com
SCIENCE DIRECT
Biochemical and Biophysical Research Communications 343 (2006) 159–166
BBRC
www.elsevier.com/locate/ybbrc

Synergistic action of Wnt and LIF in maintaining pluripotency of mouse ES cells

Kazuya Ogawa [a], Ryuichi Nishinakamura [b], Yuko Iwamatsu [a], Daisuke Shimosato [a,c], Hitoshi Niwa [a,c,*]

[a] *Laboratory for Pluripotent Cell Studies, RIKEN Center for Developmental Biology, 2-2-3 Minatojima-Minamimachi, Chuo-ku, Kobe 650-0047, Japan*
[b] *Division of Integrative Cell Biology, Institute of Molecular Embryology and Genetics, Kumamoto University, 2-2-1 Honjo, Kumamoto 860-0811, Japan*
[c] *Department of Developmental and Regenerative Medicine, Graduate School of Medicine, Kobe University, 7-5-1 Kusunokicho, Chuo-ku, Kobe 650-0017, Japan*

Received 10 February 2006
Available online 2 March 2006

Abstract

Leukaemia inhibitory factor (LIF) was the first soluble factor identified as having potential to maintain the pluripotency of mouse embryonic stem (ES) cells. Recently, a second factor, Wnt, with similar activity was found. However, the relationship between these completely different signals mediating the overlapping functions is still unclear. Here, we report that the conditioned medium of L cells expressing Wnt3a maintains ES cells in the undifferentiated state in feeder-free culture, followed by expression of stem cell markers and their ability to generate germline chimaeras. However, although the activity of this conditioned medium is dependent on Wnt3a, recombinant Wnt3a protein cannot maintain ES cells in the undifferentiated state. As supplementation with Wnt3a to the sub-threshold level of LIF alone was not sufficient to maintain ES self-renewal, the results of maintenance of the undifferentiated state indicated the synergistic action of Wnt and LIF. Induction of constitutively activated β-catenin alone is unable to maintain ES self-renewal but shows a synergistic effect with LIF. These observations indicate that the Wnt signal mediated by the canonical pathway is not sufficient but enhances the effect of LIF to maintain self-renewal of mouse ES cells.

Keywords: Embryonic stem cell; Self-renewal; Wnt; LIF; β-Catenin; BIO

Mouse ES (mES) cells can be propagated in medium containing foetal calf serum (FCS) and the cytokine, leukaemia inhibitory factor (LIF), without the support of feeder cells [1,2]. The effect of LIF is mediated through a cell-surface complex composed of LIFRβ and gp130. Upon ligand binding, gp130 activates Janus-associated tyrosine kinases (JAK) and their downstream component, signal transducer and activator of transcription (STAT)3. Activation of STAT3 is necessary and sufficient for suppression of differentiation of mES cells [3,4]. However, LIF alone is not sufficient for clonal expansion of feeder-free mES cells in the absence of serum [5] and is unable to support self-renewal of human or monkey cells without feeder layers even in the presence of serum [6,7]. These findings suggest that unidentified growth factors provided by feeder cells and serum contribute to the maintenance of the self-renewal capacity of ES cells.

Wingless/Wnts are developmentally regulated secretory proteins that control cell differentiation, movement, and proliferation. Large-scale gene expression profiling of mES cells revealed that components of several signal transduction pathways are transcriptionally enriched in the undifferentiated state, and the main components of the canonical Wnt pathway are detected in ES cells in the undifferentiated state [8]. Sato et al. [9] reported that the GSK-3 inhibitor, 6-bromoindirubin-3′-oxime (BIO), maintains the pluripotency of mES and human ES (hES) cells. However, another group reported that addition of Wnt3a stimulated not only hES cell proliferation but also

* Corresponding author. Fax: +81 78 306 1929.
E-mail address: niwa@cdb.riken.jp (H. Niwa).

0006-291X/$ - see front matter © 2006 Elsevier Inc. All rights reserved.
doi:10.1016/j.bbrc.2006.02.127

differentiation [10]. These discrepancies suggest that the canonical Wnt signal activation is not absolutely sufficient for maintenance of the pluripotency of ES cells, but that its activity is context-dependent.

In this study, we investigated the effects of the Wnt signal on mES cell self-renewal using a stem cell selection system based on Oct3/4 expression and feeder-free culture conditions [11], which allowed us to determine the direct effect of Wnt on undifferentiated ES cells.

Materials and methods

ES cell culture. ES cells were maintained on feeder-free gelatine-coated plates in FCS-containing medium supplemented with LIF: Glasgow minimal essential medium (GMEM; Sigma–Aldrich) supplemented with 10% FCS (selected batches, Sigma–Aldrich), 100 μM 2-mercaptoethanol (Nacalai Tesque), 1× non-essential amino acids (Invitrogen), 1 mM sodium pyruvate (Invitrogen), and 1000 U/ml (U) LIF (ESGRO; Invitrogen). EB3 and OLG2-3 ES cells were generated by introduction of Oct3/4 knockout vector carrying IRESBSDpA and EGFP IRES pacpA into E14TG2a ES cells by homologous recombination [11,12], and cultured in the presence of 5 μg/ml blasticidin S (Kaken Pharmaceutical) and 1.5 μg/ml puromycin (Sigma–Aldrich) for stem cell selection. For in vitro experiments, EB3, OLG2-3 or D3 ES cells were seeded onto gelatine-coated 12- or 6-well plates at a density of 3×10^2 or 1×10^3 cells/well, and cultured for 5–6 days in conditioned or non-conditioned medium, in the presence of LIF or recombinant Wnt3a (R&D Systems) or recombinant frizzled8-Fc (Fz8-Fc; R&D Systems) or anti-LIF antibody (R&D Systems), which were added to fresh medium three days later, or the GSK-3 inhibitor, 6-bromoindirubin-3′-oxime (BIO; Calbiochem). Alkaline phosphatase staining was carried out using BCIP/NBT solution (Sigma-Aldrich).

Conditioned media. L cells (1×10^6 cells) expressing mouse Wnt3a or vector alone (ATCC) were plated onto dishes 9 cm in diameter [13]. Three days later, cells were washed three times with phosphate-buffered saline (PBS) and transferred to fresh FCS-containing medium. The supernatants were collected after 3 days and used at a threefold dilution for ES cell culture. These conditioned media were designated L-Wnt3a CM and L-CM, respectively. To collect the supernatants of L cells stimulated with Wnt-3a, L cells (1×10^6 cells) were expanded in L-Wnt3a CM for 3 days, washed three times with PBS, and transferred to fresh FCS-containing medium. The supernatants were collected after 3 days and designated L(w3a) CM, and used at a threefold dilution for ES cell culture.

Generation of EBRTcPβ-cateninwt and EBRTcPβ-cateninΔGSK ES cells. β-Catenin and β-cateninΔ*GSK* cDNA were introduced into the *Xho*I and *Not*I sites of the exchange vector pPthC to obtain pPthC-β-cateninwt and pPthC-β-cateninΔ*GSK*, respectively [14,15]. EBRTcH3 ES cells were seeded onto gelatine-coated 6-well plates at a density of 1×10^5 cells/well. The next day, 0.5 μg pPthC-β-cateninwt or pPthC-β-cateninΔ*GSK* and 0.5 μg pCAGGS-Cre were co-transfected using Lipofectamine 2000 (Invitrogen). The transfected cells were re-plated onto dishes 9 cm in diameter in medium containing 1 μg Tc (Sigma–Aldrich) and transferred to medium FCS-containing 1 μg Tc and 1.5 μg/ml of puromycin. The selected recombinant cells were maintained in FCS-containing medium containing 1 μg Tc and 1.5 μg/ml of puromycin. For in vitro experiments, EBRTcPβ-cateninwt or EBRTcPβ-cateninΔGSK ES cells were seeded onto gelatine-coated 6-well plates at a density of 2×10^3 cells/well, and cultured for 5 days in FCS-containing medium, in the presence or absence of Tc or LIF, which were added to fresh medium three days later. Alkaline phosphatase staining was carried out using BCIP/NBT solution (Sigma–Aldrich).

Luciferase reporter assay. OLG2-3, EBRTcPβcateninwt, and EBRTcPβcateninΔGSK ES cells were seeded onto gelatine-coated 24-well plates at a density of 5×10^4 cells/well. The following day, cells were co-transfected with 0.5 μg of TOP-Flash or FOP-Flash reporter (Upstate) or 2 μg of 4× APRE-luc and 0.005 μg or 0.02 μg pRL-CMV (Promega) using Lipofectamine 2000 [16,17]. Luciferase activities were measured by dual luciferase assay 24 h after transfection (Promega). Luciferase activities were normalized to those of co-transfected pRL-RL.

RNA isolation, Northern blotting, and reverse transcription-polymerase chain reaction (RT-PCR) analysis. Total RNAs were prepared with TRIzol reagent (Invitrogen) according to the manufacturer's instructions. Oligo(dT)-primed cDNAs were prepared from 1 μg of total RNA using ReverTra Ace (Toyobo) and aliquots of 1/20th of the cDNA products were used for each PCR amplification. The gene-specific primers were as follows: sense primer for *H19* CAAGGTGAAGCTGAAAGAACA GATGG, antisense primer for *H19* TCCAAACCAGTGCAATCGACTT AG, sense primer for *tPA* GCCCTCTGGTGTGCATGATCAAT and antisense primer for *tPA* TTCCAAAGCCAGACCTTCATCCTT. These corresponded to the Accession Nos: J03250 (*tPA*) and X58196 (*H19*). PCR products were separated by electrophoresis on 1.2% agarose gels and visualized with ethidium bromide. For Northern blotting analysis, aliquots of 4 μg of total RNA were separated on denaturing agarose gels and then blotted onto Hybond-N membranes (Amersham Biosciences). Analyses were performed with GeneImage (Amersham Biosciences) according to the manufacturer's instructions.

Generation of chimaeric mice. EB3 cells were propagated at clonal density and maintained for more than 2 months in L-Wnt3a CM. Microinjection of ES cells into C57BL/6J blastocysts was performed according to standard procedures [18].

Western blotting analysis. For analysis of STAT3 phosphorylation, aliquots of 1×10^7 OLG2-3 ES cells were seeded onto gelatine-coated dishes 9 cm in diameter and cultured in FCS-containing medium without LIF. The next day, cells were treated with LIF or Wnt3a in FCS-containing medium for 2 h. Cells were then washed twice with ice-cold PBS and scraped off in 100 μl of ice-cold lysis buffer (50 mM Tri–HCl, pH 7.4, 1% NP-40, 0.025% sodium deoxycholate, 150 mM NaCl, 1 mM EDTA, 1 mM PMSF, 1 mM Na_3VO_4, and 1 mM NaF) containing 1% proteinase inhibitor cocktail (Sigma). Aliquots of 30 μg of total protein from each sample were separated by electrophoresis on 10% SDS–polyacrylamide gels and electroblotted onto PDF membranes (Immobilon; Nihon Millipore). After treatment in blocking buffer (10 mM Tris–HCl, pH 7.4, 137 mM NaCl, 2.7 mM KCl, 0.1% Tween 20, and 3% skimmed milk), the membranes were probed sequentially with anti-STAT3 (Cell Signaling Technology) or anti-phospho-STAT3 (705Tyr) (Cell Signaling Technology) and then with horseradish peroxidase-coupled anti-rabbit IgG (Jackson Immuno Research), developed using ECL reagents (Amersham Biosciences).

Results and Discussion

To determine whether activation of the Wnt signal is absolutely sufficient to maintain pluripotency of mES cells, we first examined the effects of conditioned medium from mouse fibroblast L cells expressing Wnt3a (L-Wnt3a CM) as a source of Wnt activity on mES self-renewal using a feeder-free culture system [11,13]. To determine the actual effect of Wnt3a in the conditioned medium on mES cells, we used two different negative controls: conditioned medium from wild-type L cells (L CM) and conditioned medium from these cells stimulated with L-Wnt3a CM (L(w3a) CM). The latter allowed us to distinguish the direct effect of Wnt3a on mES cells from its indirect effect via stimulation of L cells to produce factors that affect mES self-renewal. Monitoring of Wnt activity on mES cells by luciferase assay using TOP-Flash (TOP) and FOP-Flash (FOP) reporters revealed that only L-Wnt3a CM contained significant levels of Wnt activity sufficient to stimulate the canonical Wnt signal mediating β-catenin/T-cell-specific factor (TCF) transcriptional activity in mES cells

(Fig. 1A) [16]. In contrast, the same reporter assay revealed no detectable activation of the canonical Wnt signal in mES cells maintained by LIF, indicating that LIF does not have any cross-reactivity either directly or indirectly via activation of the autocrine loop of the Wnt signal. Functional assays of these conditioned media indicated that only L-Wnt3a CM showed the ability to maintain EB3 or OLG2-3 feeder-free ES cells in the undifferentiated

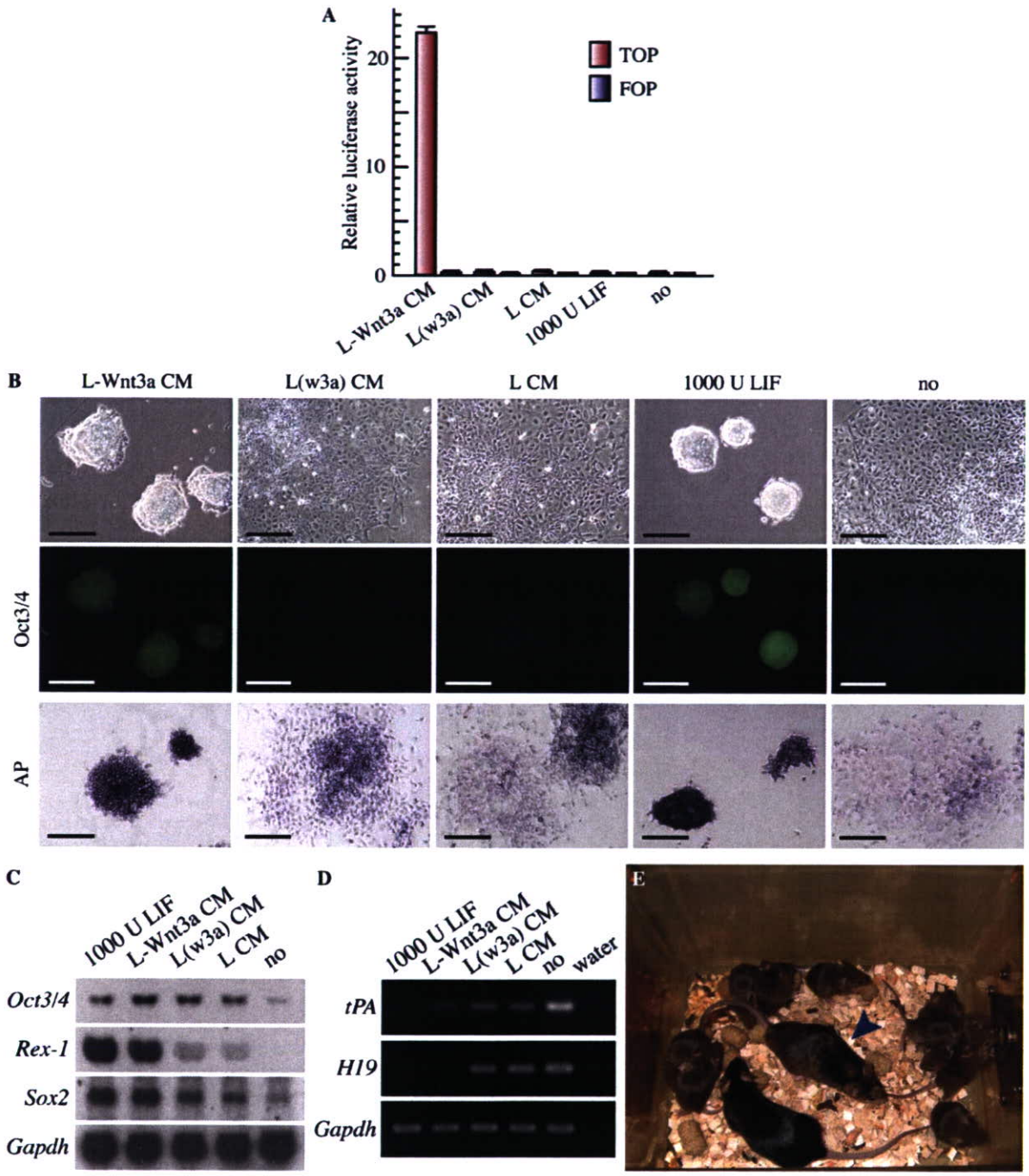

Fig. 1. L-Wnt3a CM maintains the pluripotency of mES cells. (A) Luciferase assay for TOP/FOP reporters in OLG 2-3 ES cells. Each bar represents the mean ± SEM ($n = 3$). (B) Colony morphologies of OLG2-3 and EB3 ES cells. OLG2-3 (upper and middle) or EB3 (lower) cells were cultured in L-Wnt3a CM, L(w3a)CM, L CM, or FCS-containing medium supplemented with or without LIF for 5 days. The middle panel shows expression of Oct3/4-EGFP and the lower panel shows AP-staining as markers of the undifferentiated state. Scale bars, 200 μm. (C) Expression of stem cell marker genes *Oct3/4*, *Sox2*, and *Rex1* in OLG2-3 ES cells cultured in L-Wnt3a CM, L(w3a)CM, L CM or FCS-containing medium supplemented with or without LIF for 5 days examined by Northern blotting analysis. *Gapdh* was used as a loading control. (D) Expression of differentiated cell marker genes in OLG2-3 ES cells analysed by RT-PCR. *Gapdh* was used as loading control. (E) Germline-competent male chimaeric mice (arrowhead) derived from EB3 cells cultured with L-Wnt3a CM for at least 2 months, and mated with female C57BL/6J mice, resulting in Agouti pups.

state, as determined by the compact colony morphology as well as the expression of Oct3/4 or alkaline phosphatase (AP) activity, comparable to that of medium containing 1000 U/ml (U) of recombinant LIF (Fig. 1B). Another cell line, D3 ES cells, can also be maintained in L-Wnt3a CM (Fig. 2D). Maintenance of the undifferentiated state and prevention of differentiation were confirmed by the expression of marker genes, and stem cell markers, such as *Oct3/4*, *Rex1*, and *Sox2*, were maintained (Fig. 1C), while differentiation markers, such as *tPA* and *H19*, were suppressed in ES cells maintained in L-Wnt3a CM (Fig. 1D) [11,19,20]. Finally, the appropriate maintenance of pluripotency in L-Wnt3a CM was confirmed by generation of germline-competent chimaeric mice by injection of EB3 ES cells maintained in L-Wnt3a CM for over 2 months (Fig. 1E). These results indicated that L-Wnt3a CM is absolutely sufficient to maintain pluripotency of mES cells and that Wnt3a in L-Wnt3a CM contributes directly to this effect.

Next, we examined the effect of Wnt3a on mES cells as distinct from that of L-Wnt3a CM. First, we evaluated the contribution of Wnt3a to the effect of L-Wnt3a CM by withdrawal of its activity using soluble frizzled receptor, Fz8-Fc, a specific Wnt antagonist. Although the almost complete blockage of Wnt3a activity by Fz8-Fc was monitored by TOP/FOP reporter assay (Fig. 2A), we found that the effect of Fz8-Fc on ES self-renewal maintained by L-Wnt3a CM was weaker than that of complete replacement of L-Wnt3a CM with L CM (Figs. 1B and 2B), suggesting that not only Wnt3a but also another factor(s) contributes to the ability of L-Wnt3a CM to maintain ES self-renewal. As LIF is the most potent factor to maintain pluripotency of mES cells, we tested the activity of LIF in Wnt3a CM by LIF-dependent reporter assay. Experiments using a STAT3-responsive reporter 4×acute phase response element (APRE)-luc indicated that Wnt3a CM contains LIF activity comparable to that of 10 U of recombinant LIF (Fig. 3C) [17]. The concentration of LIF in L-Wnt3a CM was estimated as 60 pg/ml (about 6 U) by enzyme immunoassay, whereas that in L CM was 20 pg/ml (about 2 U). Neutralization of LIF activity in L-Wnt3a CM by addition of anti-LIF antibody resulted in its reduced ability to maintain self-renewal (Fig. 3D). These observations suggested that L-Wnt3a CM may maintain the pluripotency of mES cells via the synergistic action of Wnt3a and LIF.

The synergistic action of Wnt3a and LIF on mES self-renewal was evaluated by addition of each recombinant protein to serum-containing medium. Activation of STAT3 by phosphorylation on 705Tyr was reported to be necessary and sufficient to maintain pluripotency of mES cells [3]. Addition of recombinant Wnt3a resulted in activation of the canonical Wnt signal monitored by TOP/FOP reporters comparable to that by L-Wnt3a CM (Fig. 3A), but had no effect on STAT3 phosphorylation (Fig. 3B), whereas recombinant LIF stimulated STAT3 phosphorylation in a dose-dependent manner without activation of the canonical Wnt signal (Figs. 3A and B). These observations indicated that there is no cross-effect between these two ligands. Various concentrations of LIF were examined

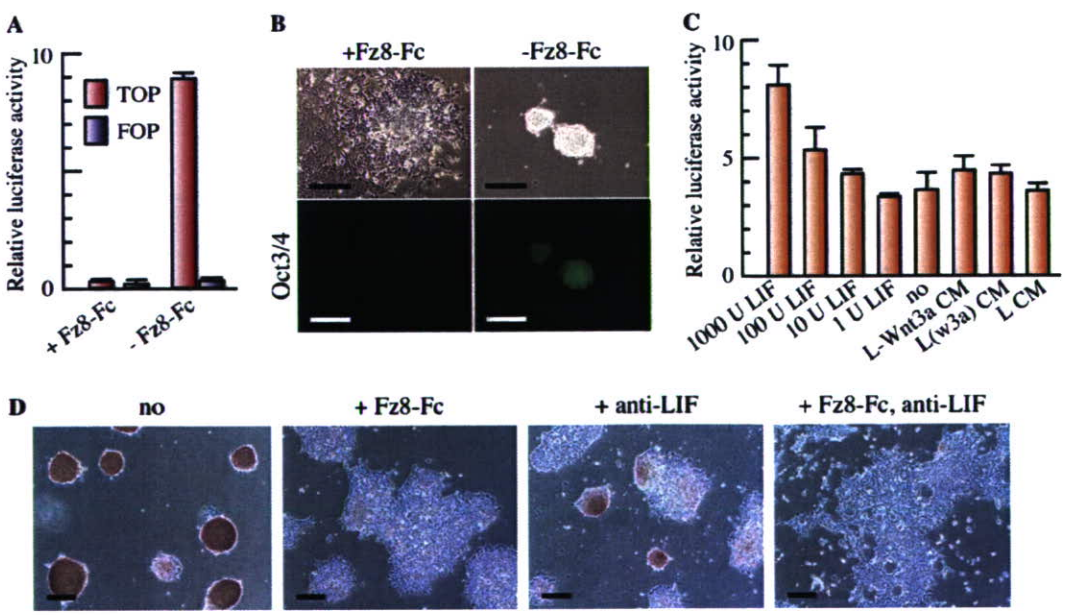

Fig. 2. Synergistic effect between Wnt and LIF signal in L-Wnt3a CM. (A) Luciferase assay for TOP/FOP reporters in OLG 2-3 ES cells. Each bar represents the mean ± SEM ($n = 3$). (B) Effects of antagonists against Wnt (1 μg/ml mouse Fz8-Fc) on self-renewal of OLG2-3 ES cells cultured in L-Wnt3a CM. ES cells were cultured in L-Wnt3a CM supplemented with (left) or without Fz8-Fc (right) for 5 days. The lower panel shows expression of Oct3/4-EGFP. Scale bars, 200 μm. (C) Luciferase assay for 4 × APRE-luc in OLG2-3 ES cells. (D) Effects of antagonists against Wnt (1 μg/ml mouse Fz8-Fc) and/or LIF (1 μg/ml anti-LIF antibody) on self-renewal of D3 ES cells cultured in L-Wnt3a CM. D3 ES cells were cultured in L-Wnt3a CM supplemented with Fz8-Fc and/or anti-LIF antibody or with no additional factors for 6 days. AP staining shows undifferentiated D3 ES cells.

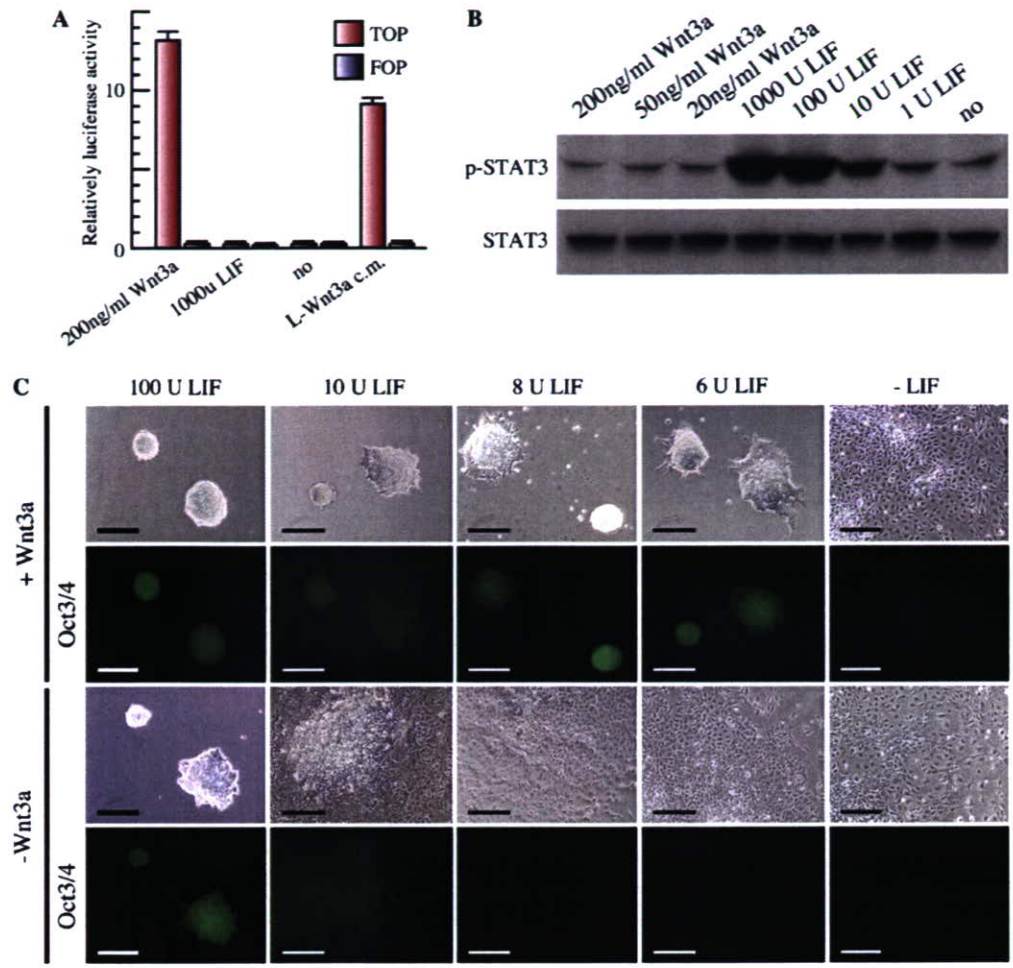

Fig. 3. Synergistic effect between Wnt3a protein and LIF on mES cell self-renewal. (A) Luciferase assay for TOP/FOP reporters in OLG2-3 ES cells. Each bar represents the mean ± SEM ($n = 3$). (B) Effects of Wnt3a protein on STAT3 phosphorylation in OLG2-3 ES cells. EB5 cells were treated with Wnt or LIF at the indicated concentration for 2 h and subjected to Western blotting analysis using anti-phospho-STAT3 (705Tyr) antibody (upper panel) and anti-STAT3 antibody (lower panel). (C) Colony morphologies of OLG2-3 ES cells. OLG2-3 cells were cultured in FCS-containing medium supplemented with or without 200 ng/ml Wnt3a at various concentrations of LIF for 5 days. The second and fourth panels show expression of Oct3/4-EGFP. Scale bars, 200 μm.

for their abilities to maintain mES cells in the undifferentiated state. Our results indicated that 10 U was the minimal dose to give Oct3/4-positive stem cell colonies (Fig. 3C). In contrast, if recombinant Wnt3a was added simultaneously with LIF, 6 U of LIF was sufficient to support Oct3/4-positive colony formation (Fig. 3C), indicating that Wnt3a can reduce the requirement for LIF to maintain self-renewal. However, Oct3/4-positive colonies could not be generated in medium containing Wnt3a without LIF (Fig. 3C), indicating that Wnt3a alone is not sufficient to maintain ES self-renewal but that it acts synergistically with LIF.

These observations raise the question of how the synergistic action of Wnt3a and LIF is mediated. To assess the contribution of the canonical Wnt signal to this phenomenon, we examined the effect of direct activation of this signal by accumulation of β-catenin in ES cells. For this purpose, we introduced tetracycline-regulatable transgenes for expression of either wild-type (wt) or the constitutively active form of β-catenin, which carries four point mutations (S33A, S37A, T41A, and S45A) at the GSK-binding site to prevent the interaction [14,15]. The effect of β-catenin ΔGSK overexpression on the canonical Wnt signal was confirmed by TOP/FOP reporters, which was comparable to the effect mediated by L-Wnt3a CM (Fig. 4A). The effects of overexpression of β-catenin wt and β-catenin ΔGSK to support self-renewal, and we detected their synergistic activities with sub-threshold levels of LIF to maintain the cells in the undifferentiated state (Fig. 4B). Moreover, as shown in the case of recombinant Wnt3a, direct activation of the canonical Wnt signal alone was not sufficient to maintain ES self-renewal. These results suggested that the canonical Wnt signal acts synergistically with the LIF signal.

Sato et al. [9] reported that the GSK3β-specific inhibitor, BIO, can replace the activity of L-Wnt3a to maintain ES self-renewal. Therefore, we examined its effect using our feeder-free ES cell culture system as described for L-Wnt3aCM and recombinant Wnt3a. Interestingly, addition of BIO to

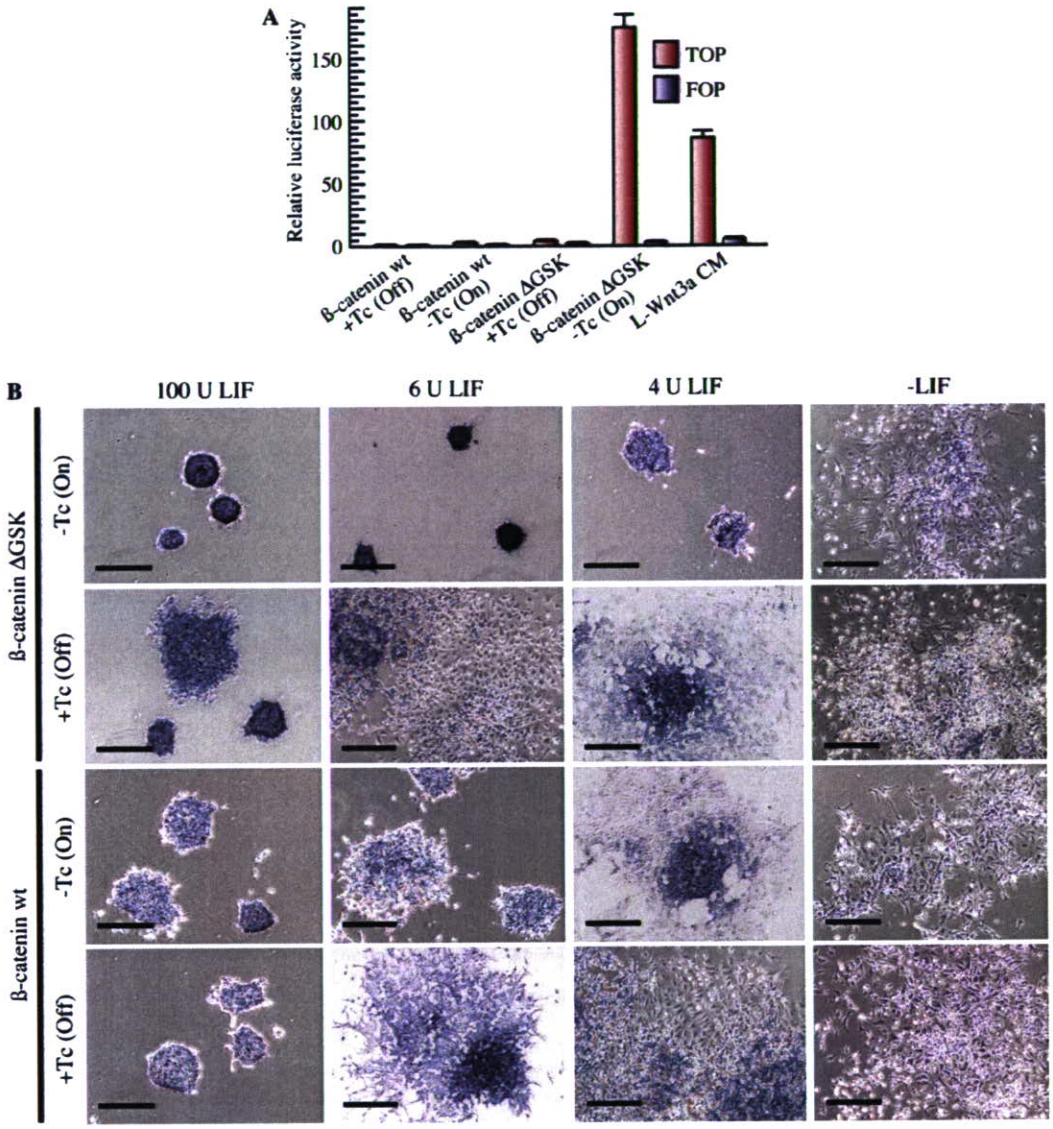

Fig. 4. Synergistic effect between constitutively activated β-catenin induction and LIF on mES cell self-renewal. (A) Luciferase assay for TOP/FOP reporters in EBRTcPβ-catenin wt and EBRTcPβ-cateninΔGSK ES cells. Each bar represents the mean ± SEM ($n = 3$). (B) AP-stained colony morphologies of EBRTcPβ-catenin wt (upper panel) and EBRTcPβ-cateninΔGSK (lower panel) ES cells. Both ES cells were cultured in FCS-containing medium supplemented with or without Tc at various concentrations of LIF for 5 days. Withdrawal of Tc (top and third panels) induced expression of β-catenin wt and β-catenin ΔGSK. Scale bars, 200 μm.

FCS-containing medium resulted in not only strong activation of the canonical Wnt signal as determined using TOP/FOP reporters (Fig. 5A), but also generation of Oct3/4-positive colonies in the absence of LIF, although the colony size was smaller than that supported by LIF for the same period (Fig. 5C). The effect of BIO on the LIF signal was estimated using APRE-luc, and the results indicated that BIO activated its expression to the same level as that induced by 100 U LIF (Fig. 5B). Although the molecular mechanism of this effect remains unclear, maintenance of ES self-renewal by BIO may be due to its combinatorial effect in activating both the canonical Wnt signal and the LIF signal simultaneously, as in the case of L-Wnt3a CM and the combination of recombinant Wnt3a and LIF.

The results of the present study indicated that addition of recombinant Wnt3a protein and induction of constitutively activated β-catenin maintain the pluripotency of mES cells by cooperation with sub-threshold levels of LIF, but that they were not sufficient to maintain self-renewal of mES cells in the absence of LIF. Our findings in mES cells were consistent with those in mouse haematopoietic stem (HS) cells, for which Wnt3a by cooperation with Steel locus factor (SLF) has been shown to support stem cell self-renewal [21]. These findings indicate that the function of the Wnt signal is limited to a supportive effect for the maintenance of the pluripotency of mES cells.

We found that BIO maintained the undifferentiated state of a subset of mES cells and induced differentiation

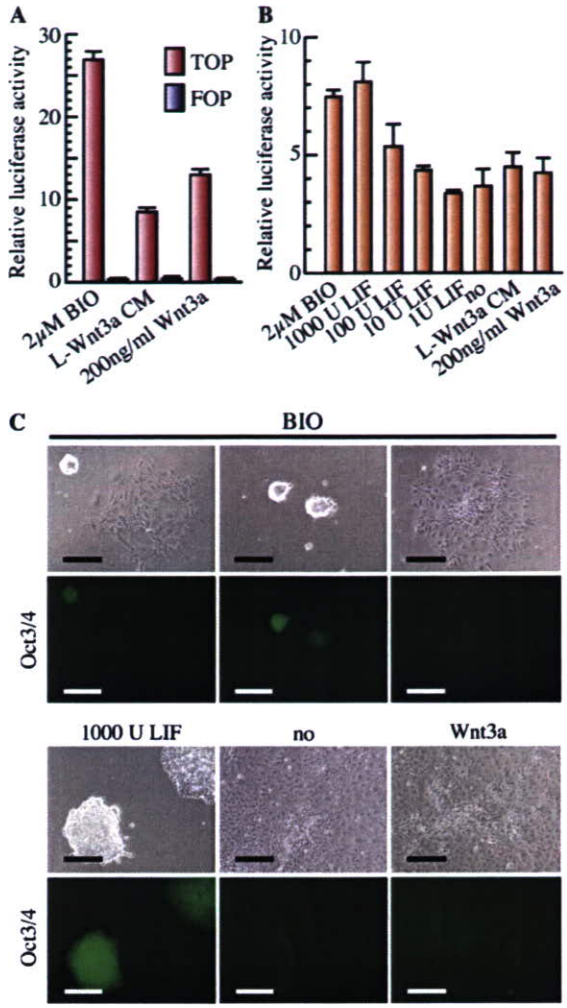

Fig. 5. Synergistic effect between Wnt and LIF signal by BIO. (A) Luciferase assay for TOP/FOP reporters in OLG 2-3 ES cells. (B) Luciferase assay for 4× APRE reporters in OLG 2-3 ES cells. Each bar represents the mean ± SEM ($n = 3$). (C) Effects of BIO on OLG2-3 ES cell self-renewal. ES cells were cultured in FCS-containing medium supplemented with 2 μM BIO, 1000 U LIF, 200 ng/ml Wnt3a or no factor for 6 days. The lower panel shows expression of Oct3/4-EGFP. Scale bars, 200 μm.

of the remaining cells with activation of STAT3-specific reporter. The variation of responsiveness of mES cells to BIO may reflect the heterogeneity of Oct3/4-positive mES cells in which different subpopulations show various capabilities of signal integration [22]. Our results suggest that BIO may have combinatorial effects on mES cells, activating both the canonical Wnt signal and the LIF signal simultaneously to maintain the cells in the undifferentiated state, as in the case of the combination of recombinant Wnt3a and LIF. We could not evaluate the mechanism by which BIO activates STAT3 transcriptional activity as there is no evidence of a connection between GSK3 and the LIF-Jak-STAT3 signal cascade.

It was reported recently that recombinant Wnt3a alone is not sufficient to maintain human ES cells in the undifferentiated state, although L-Wnt3a CM can do so [9,10]. These findings were similar to our observations in mES cells, indicating that factor(s) in L-Wnt3a CM act synergistically with Wnt. However, it was also reported that activation of STAT3 is neither sufficient nor necessary to maintain self-renewal of hES cells. Therefore, the LIF-STAT3 signal should not be a partner of Wnt for its synergistic action. We are currently attempting to identify the unknown partner(s) of Wnt for human ES cells, which may be activated by BIO, as it is sufficient to maintain the undifferentiated state in a limited period.

Acknowledgments

We thank Dr. Shinji Masui (RIKEN CDB) for technical suggestions regarding the ROSA-TET expression system. This work was supported in part by a Grant-in-Aid for Scientific Research from the Ministry of Education, Science, Culture of Japan (to H.N.), the Ministry of Health, Labor and Welfare of Japan (to R.N.), and Leading Project (to H.N.).

References

[1] A.G. Smith, J.K. Heath, D.D. Donaldson, G.G. Wong, J. Moreau, M. Stahl, D. Rogers, Inhibition of pluripotential embryonic stem cell differentiation by purified polypeptides, Nature 336 (1988) 688–690.
[2] H. Niwa, Molecular mechanism to maintain stem cell renewal of ES cells, Cell Struct. Funct. 26 (2001) 137–148.
[3] H. Niwa, T. Burdon, I. Chambers, A.G. Smith, Self-renewal of pluripotent embryonic stem cells is mediated via activation of STAT3, Genes Dev. 12 (1998) 2048–2060.
[4] T. Matsuda, T. Nakamura, K. Nakao, T. Arai, M. Katsuki, T. Heike, T. Yokota, STAT3 activation is sufficient to maintain an undifferentiated state of mouse embryonic stem cells, EMBO J. 18 (1999) 4261–4269.
[5] K. Ogawa, H. Matsui, S. Ohtsuka, H. Niwa, A novel mechanism for regulating clonal propagation of mouse ES cells, Genes Cells 9 (2004) 471–477.
[6] J.A. Thomson, J. Itskovitz-Eldor, S.S. Shapiro, M.A. Waknitz, J.J. Swiergiel, V.S. Marshall, J.M. Jones, Embryonic stem cell lines derived from human blastocysts, Science 282 (1998) 1145–1147.
[7] H. Suemori, T. Tada, R. Torii, Y. Hosoi, K. Kobayashi, H. Imahie, Y. Kondo, A. Iritani, N. Nakatsuji, Establishment of embryonic stem cell lines from cynomolgus monkey blastocysts produced by IVF or ICSI, Dev. Dyn. 222 (2001) 273–279.
[8] N. Sato, I.M. Sanjuan, M. Heke, M. Uchida, F. Naef, A.H. Brivanlou, Molecular signature of human embryonic stem cells and its comparison with the mouse, Dev. Biol. 260 (2003) 404–413.
[9] N. Sato, L. Meijer, L. Skaltsounis, P. Greengard, A.H. Brivanlou, Maintenance of pluripotency in human and mouse embryonic stem cells through activation of Wnt signaling by a pharmacological GSK-3-specific inhibitor, Nat. Med. 10 (2004) 55–63.
[10] G. Dravid, Z. Ye, H. Hammond, G. Chen, A. Pyle, P. Donovan, X. Yu, L. Cheng, Defining the role of Wnt/beta-catenin signaling in the survival, proliferation, and self-renewal of human embryonic stem cells, Stem Cells 23 (2005) 1489–1501.
[11] H. Niwa, S. Masui, I. Chambers, A.G. Smith, J. Miyazaki, Phenotypic complementation establishes requirements for specific POU domain and generic transactivation function of Oct-3/4 in embryonic stem cells, Mol. Cell. Biol. 22 (2002) 1526–1536.
[12] M. Hooper, K. Hardy, A. Handyside, S. Hunter, M. Monk, HPRT-deficient (Lesch-Nyhan) mouse embryos derived from germline colonization by cultured cells, Nature 326 (1987) 292–295.

[13] S. Shibamoto, K. Higano, R. Takada, F. Ito, M. Takeichi, S. Takada, Cytoskeletal reorganization by soluble Wnt-3a protein signalling, Genes Cells 3 (1998) 659–670.
[14] A.I. Barth, D.B. Stewart, W.J. Nelson, T cell factor-activated transcription is not sufficient to induce anchorage-independent growth of epithelial cells expressing mutant beta-catenin, Proc. Natl. Acad. Sci. USA 96 (1999) 4947–4952.
[15] S. Masui, D. Shimosato, Y. Toyooka, R. Yagi, K. Takahashi, H. Niwa, An efficient system to establish multiple embryonic stem cell lines carrying an inducible expression unit, Nucleic Acids Res. 33 (2005) e43.
[16] M.P. Coghlan, A.A. Culbert, D.A. Cross, S.L. Corcoran, J.W. Yates, N.J. Pearce, O.L. Rausch, G.J. Murphy, P.S. Carter, L. Roxbee Cox, D. Mills, M.J. Brown, D. Haigh, R.W. Ward, D.G. Smith, K.J. Murray, A.D. Reith, J.C. Holder, Selective small molecule inhibitors of glycogen synthase kinase-3 modulate glycogen metabolism and gene transcription, Chem. Biol. 7 (2000) 793–803.
[17] T. Takeda, H. Kurachi, T. Yamamoto, H. Homma, K. Adachi, K. Morishige, A. Miyake, Y. Murata, Alternative signaling mechanism of leukemia inhibitory factor responsiveness in a differentiating embryonal carcinoma cell, Endocrinology 138 (1997) 2689–2696.
[18] B. Hogan, R. Beddington, F. Constantini, E. Lacy, Manipulating the Mouse Embryo, Cold Spring Harbor Laboratory Press, New York, 1994.
[19] H. Niwa, J. Miyazaki, A.G. Smith, Quantitative expression of Oct-3/4 defines differentiation, dedifferentiation or self-renewal of ES cells, Nat. Genet. 24 (2000) 372–376.
[20] J. Fujikura, E. Yamato, S. Yonemura, K. Hosoda, S. Masui, K. Nakao, J. Miyazaki Ji, H. Niwa, Differentiation of embryonic stem cells is induced by GATA factors, Genes Dev. 16 (2002) 784–789.
[21] K. Willert, J.D. Brown, E. Danenberg, A.W. Duncan, I.L. Weissman, T. Reya, J.R. Yates 3rd, R. Nusse, Wnt proteins are lipid-modified and can act as stem cell growth factors, Nature 423 (2003) 448–452.
[22] T. Furusawa, K. Ohkoshi, C. Honda, S. Takahashi, T. Tokunaga, Embryonic stem cells expressing both platelet endothelial cell adhesion molecule-1 and stage-specific embryonic antigen-1 differentiate predominantly into epiblast cells in a chimeric embryo, Biol. Reprod. 70 (2004) 1452–1457.

Development 133, 3005-3013 (2006) doi:10.1242/dev.02457

The murine homolog of *SALL4*, a causative gene in Okihiro syndrome, is essential for embryonic stem cell proliferation, and cooperates with *Sall1* in anorectal, heart, brain and kidney development

Masayo Sakaki-Yumoto[1,*], Chiyoko Kobayashi[1,*], Akira Sato[2], Sayoko Fujimura[1], Yuko Matsumoto[2], Minoru Takasato[3], Tatsuhiko Kodama[4], Hiroyuki Aburatani[4], Makoto Asashima[3], Nobuaki Yoshida[5] and Ryuichi Nishinakamura[1,2,6,*,†]

Mutations in *SALL4*, the human homolog of the *Drosophila* homeotic gene *spalt* (*sal*), cause the autosomal dominant disorder known as Okihiro syndrome. In this study, we show that a targeted null mutation in the mouse *Sall4* gene leads to lethality during peri-implantation. Growth of the inner cell mass from the knockout blastocysts was reduced, and *Sall4*-null embryonic stem (ES) cells proliferated poorly with no aberrant differentiation. Furthermore, we demonstrated that anorectal and heart anomalies in Okihiro syndrome are caused by *Sall4* haploinsufficiency and that *Sall4/Sall1* heterozygotes exhibited an increased incidence of anorectal and heart anomalies, exencephaly and kidney agenesis. Sall4 and Sall1 formed heterodimers, and a truncated Sall1 caused mislocalization of Sall4 in the heterochromatin; thus, some symptoms of Townes-Brocks syndrome caused by SALL1 truncations could result from SALL4 inhibition.

KEY WORDS: *Sall4*, *spalt*, Embryonic stem cells, Okihiro syndrome, Townes-Brocks syndrome, Organogenesis, Mouse

INTRODUCTION

Early differentiation of the mammalian embryo leads to the development of two distinct lineages – the inner cell mass (ICM) and the trophectoderm. Cells of the ICM are pluripotent and give rise to the epiblast and eventually to all the fetal tissues, while trophectoderm cells have restricted potential and give rise to the trophoblast cell layers of the placenta. Embryonic stem (ES) cells are established from the ICM and have the potential to generate chimeric mice when introduced into a blastocyst. When cultured in vitro, ES cells differentiate into a variety of cell lineages; thus, human ES cells are possible candidates for cell therapies, although there are some ethical issues to overcome. Maintenance of mouse ES cell pluripotency requires constant suppression of their differentiation by both extrinsic and intrinsic factors. Leukemia inhibitory factor (LIF) and bone morphogenetic protein 4 (BMP4) are the two major extrinsic signals (Niwa et al., 1998; Matsuda et al., 1999; Ying et al., 2003). LIF induces phosphorylation and nuclear localization of STAT3, a transcription factor essential for the LIF-dependent pathway for self-renewal. BMP4 induces phosphorylation and nuclear localization of Smad1, and the subsequent upregulation of Id helix-loop-helix proteins that block neural differentiation and maintain the pluripotency of ES cells in the presence of the LIF signal. Intrinsic factors include *Oct3/4*, *Nanog* and *Eras*. *Oct3/4* and *Nanog* are expressed at high levels in ES cells and have been shown to be essential for maintaining pluripotency in ES cells (Chambers et al., 2003; Mitsui et al., 2003; Nichols et al., 1998). *Eras* and *Utf1* are also expressed abundantly in ES cells, and they play crucial roles in the proliferation of stem cells (Takahashi et al., 2003; Nishimoto et al., 2005).

The *spalt* (*sal*) gene was first isolated from *Drosophila* and it encodes a protein characterized by multiple double zinc-finger motifs of the C2H2 type. *sal* acts as a region-specific homeotic gene, and is required for the specification of the head and tail regions during early development (Jurgens, 1988; Kuhnlein et al., 1994). During the later stages of development, *sal* regulates pattern formation and cell fate decisions in the wing disc (de Celis et al., 1996; Nellen et al., 1996), trachea (Kuhnlein and Schuh, 1996) and sensory organ development (de Celis et al., 1999). *sal* is expressed at the anteroposterior boundary of the wing imaginal discs, and its expression is controlled by the *dpp* (decapentaplegic) gene (de Celis et al., 1996; Nellen et al., 1996).

Humans and mice each have four known Sal-related genes (known as *SALL1-SALL4* in humans and *Sall1-Sall4* in mice). Mutations in *SALL1* on chromosome 16q12.1 have been associated with Townes-Brocks syndrome, an autosomal dominant disease characterized by dysplastic ears, a preaxial polydactyly, imperforate anus and, less commonly, kidney and heart anomalies (Kohlhase et al., 1998). Mice deficient in *Sall1* show kidney agenesis or severe dysgenesis, but other phenotypes observed in the human disease are not apparent (Nishinakamura et al., 2001). This discrepancy could be explained by the formation of truncated SALL1 proteins as a result of mutations in *SALL1*, as comparison with *Sall1*-null mice showed that mutant mice producing a truncated Sall1 protein exhibited more severe defects, including renal agenesis, exencephaly, as well as limb and anal deformities (Kiefer et al., 2003). It has been reported that Sall1 also functions as a

[1]Division of Integrative Cell Biology, Institute of Molecular Embryology and Genetics, Kumamoto University, Kumamoto 860-0811, Japan. [2]Division of Stem Cell Regulation, The Institute of Medical Science, The University of Tokyo, Tokyo 108-8639, Japan. [3]Graduate School of Sciences, The University of Tokyo, Tokyo 113-8654, Japan. [4]Research Center for Advanced Science and Technology, The University of Tokyo, Tokyo 153-8904, Japan. [5]Laboratory of Gene Expression and Regulation, The Institute of Medical Science, The University of Tokyo, Tokyo 108-8639, Japan. [6]PRESTO, JST, Saitama 332-0012, Japan.

*These authors contributed equally to this work
†Author for correspondence (e-mail: ryuichi@kaiju.medic.kumamoto-u.ac.jp)

Accepted 24 May 2006

transcriptional repressor by localizing in the heterochromatin and interacting with components of chromatin remodeling complexes such as histone deacetylase (HDAC)1, HDAC2, retinoblastoma-associated protein 46/48 (RbAp46/48), metastasis-associated protein (MTA)1 and MTA2 (Kiefer et al., 2002).

It is still unclear if *SALL2* is associated with human disease; however, it has been reported that Sall2 functions as a tumor suppressor (Li et al., 2001; Li et al., 2004). *Sall2*-deficient mice show no apparent phenotype, and mice lacking both *Sall1* and *Sall2* show kidney phenotypes comparable with those of *Sall1* knockout mice (Sato et al., 2003). Although no diseases are thus far directly linked to *SALL3*, this gene is located in a region that is commonly deleted in cases of 18q deletion syndrome (Kohlhase et al., 1999). Individuals with this deletion exhibit hearing loss, cardiac problems, mental retardation, midfacial hypoplasia, delayed growth and limb abnormalities (Strathdee et al., 1997). *Sall3*-null mice die on the first postnatal day and deficiencies in the cranial nerves and abnormalities in the oral structures are present (Parrish et al., 2004). Mutations in *SALL4* cause an autosomal dominant disorder known as Okihiro syndrome, which is characterized by limb deformity, eye movement deficits and, less commonly, anorectal, ear, heart and kidney anomalies (Al-Baradie et al., 2002; Kohlhase et al., 2002).

To investigate the roles of Sall family genes and their functional redundancy in organogenesis, we generated *Sall4*-deficient mice. In this study, we report that the mouse *Sall4* gene was found to be unexpectedly essential for early embryogenesis, and for the proliferation of ES cells. We further reveal the importance of the heterodimerization of Sall4 and Sall1 in vivo, which could explain the underlying genetic mechanisms involved in Townes-Brocks syndrome that is caused by truncations of SALL1.

MATERIALS AND METHODS

Generation of *Sall4*-deficient mice (*Sall4-del*)

A *Sall4*-targeting vector was constructed by incorporating the 5′ *Aor51*HI-*Eco*RI 8.2-kb *Sall4* fragment and the 3′ *Bam*HI-*Eco*RV 2.3 kb fragment into a vector that contained the β-galactosidase gene (*lacZ*), the neomycin resistance (*Neo*^{r}) gene (pGK-Neo) and the diphtheria toxin A subunit (pMC1DTA) in tandem. This construct deletes all the eight zinc-finger domains of *Sall4* and results in the fusion of 39 amino acids at the N terminal of Sall4 and β-galactosidase (Fig. 1A). This strategy is identical to the one we used to delete *Sall1* (Nishinakamura et al., 2001). Five out of 114 G418-resistant E14.1 ES clones were correctly targeted and two were used to generate germline chimeras that were bred with C57BL/6J females. E14.1 ES cells were maintained on mitomycin C-treated primary embryonic fibroblasts in the presence of LIF (10^3 U/ml) and serum in all the procedures and experiments described in this paper. The primer sequences used for genotyping were as follows: 5′-GAGGACTCCATACCGGTGAA-3′, 5′-GTGCCCAGCTTCTTCAAGTC-3′ and 5′-CCTCTTCGCTATTACG-CCAG-3′ (the length of the amplified segment was 272 bp in the wild-type allele and 379 bp in the mutated allele). As the *Sall4*-deficient mice (*Sall4-del*) lacked proper *lacZ* expression, we also generated mice using the *Sall4-IRES-β-geo* vector described below.

Targeted disruption of both alleles of *Sall4*

The *Sall4-IRES β-geo* vector was constructed by incorporating the 5′ *Pac*I-*Eco*RI 4.2 kb fragment, the *Eco*RI-*Sal*I 6.0 kb *IRES-β-geo* fragment and the 3′ *Apa*LI-*Eco*RV 6.0 kb fragment into a vector that contained pMC1DTA (see Fig. S1 in the supplementary material). The *Sall4-IRES-Hyg* vector was generated by a similar method. These vectors confer drug resistance only when they are incorporated into the promoter regions of genes that are expressed in ES cells, including *Sall4* (thus facilitating the isolation of homologous recombinants). Indeed, when tested in wild-type ES cells, homologous recombinants were obtained at a frequency of 68.8% (11/16) by using the *Sall4-IRES-β-geo* vector and at 66.7% (8/12) with the *Sall4-IRES-Hyg* vector. The *Sall4-IRES-β-geo* clones were used to generate another strain of mice (*Sall4-βgeo*) for monitoring *Sall4* expression, as shown in Fig. 4D,E. This strain showed phenotypes identical to the original *Sall4*-deficient mice (*Sall4-del*).

Generation of a *Sall4* floxed allele

The *Sall4*-flox vector was constructed by incorporating the 5′ *Hin*dIII-*Hin*dIII 3.5 kb fragment, the *Hin*dIII-*Apa*LI 4.7 kb fragment and the 3′ *Apa*LI-*Eco*RV 6.0 kb fragment into a vector that contained pGK-Neo flanked by Frt and loxP sequences and pMC1DTA (see Fig. S1 in the supplementary material). LoxP sequences were placed so that exon 2 and 3 were excised upon Cre treatment, resulting in disruption of all zinc-finger motifs. Five out of 170 clones were correctly targeted (flox/+) and one of them was further transfected with the *Sall4-IRES-Hyg* vector. Both resulting

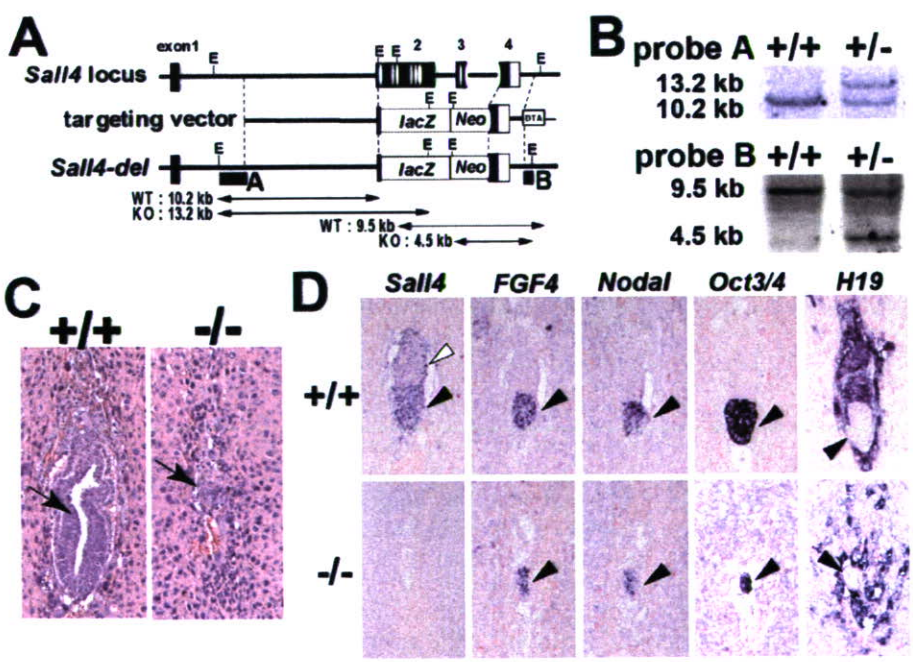

Fig. 1. Embryonic lethality of *Sall4*-deficient mice. (**A**) Targeting strategy of *Sall4*. Ovals represent the zinc-finger domains. E, *Eco*RI. (**B**) Southern blot analysis using the probes described in Fig. 1A. (**C**) Hematoxylin and Eosin staining of wild-type (+/+) and *Sall4*-deficient (–/–) embryos at E6.5. Arrow indicates epiblast. (**D**) In situ hybridization of *Sall4*, epiblast markers (*Fgf4*, *Nodal* and *Oct3/4*), and a marker for trophectoderm and extra-embryonic ectoderm (*H19*) in wild-type (+/+) and *Sall4*-deficient (–/–) embryos at E5.8. H19 signal is absent in the epiblast of both +/+ and –/– embryos. Black arrowhead, epiblast; white arrowhead, extra-embryonic ectoderm. Serial sections from two wild-type and two *Sall4*-deficient embryos are shown. Left three columns and right two comuln are from different embryos.

clones, flox/– and +/–, proliferated normally. Neo^r placed in intron 2 did not affect Sall4 expression as shown in Fig. 3C. These ES cells were infected with adenovirus expressing Cre under the CAG promoter (AxCANCre provided by RIKEN Bioresource Center) (Niwa et al., 1991; Kim et al., 2002) at a m.o.i (multiplicity of infection) of 50. After incubation for 1 hour, cells were diluted and plated onto 6-well plates coated with mitomycin C-treated embryonic fibroblasts.

Histology and blastocyst culture

Histological examination was performed as described earlier (Nishinakamura et al., 2001). In situ hybridization was performed using the AmpMap Kit and an automated Discovery System (Ventana) according to the manufacturer's protocols. Blastocyst culture and immunosurgery were also performed as described earlier (Nichols et al., 1998). cDNA was synthesized using SuperScript III CellsDirect cDNA Synthesis System (Invitrogen). Primer sequences used for RT-PCR are available upon request. 5-Bromo-2′-deoxyuridine (BrdU) labeling and detection kit I (Roche) was used to examine proliferation of the blastocysts upon 30 minutes of BrdU incorporation.

Chimera formation

Two independent *Sall4*-deficient clones were transfected with *pCAG-GFP-IRES-puro* and selected on puromycin-resistant embryonic fibroblasts (Tucker et al., 1997). Cells retaining ubiquitous green fluorescent protein (GFP) expression from each *Sall4*-deficient clone were injected into blastocysts, and consistent results were obtained. Frozen sections of the chimeras were stained by an anti-GFP antibody (Molecular Probes) and detected using ImmunoPure metal enhanced DAB substrate kit (Pierce).

Proliferation and rescue analysis of ES cells

For the proliferation assay, 1×10^4 cells were plated per well in 24-well plates in triplicate on mitomycin C-treated primary embryonic fibroblasts in media containing LIF and serum, and passaged at the same density every 4 days for 16 days to determine the cumulative cell number. A BrdU Flow Kit (BD Biosciences) was used for cell cycle analysis of ES cells after 2 hour incorporation of BrdU. For rescue analysis, the *Sall4* expression vector (*Sall4* in *pCAG-IRES-puro*) or *GFP* expression vector (negative control) was introduced into *Sall4*-deficient cells by electroporation. Multiple clones were selected on puromycin-resistant embryonic fibroblasts and expanded.

siRNA transfection

The siRNA duplexes were designed to target the coding region of mouse *Sall4* cDNA at nucleotide 2761-2785 and synthesized by Invitrogen. Sall4-siRNA or control siRNA containing the same GC content was transfected into D3 embryonic stem cells using Lipofectamine2000 (Invitrogen) according to the manufacturer's instruction, except for the maintenance of D3 cells, which were cultured on gelatin-coated plates in the presence of LIF. D3 cells at a density of 1×10^4 cells per well in 24-well plates were transfected in triplicate with 25 pmol siRNA, and counted every day. The negative control siRNA showed no growth or morphological impairment compared with the mock-transfected or the non-transfected cells.

Immunocytochemistry and confocal microscopy

The anti-Sall1 monoclonal antibody (Sato et al., 2004) and an anti-Sall4 polyclonal antibody raised against polypeptide (MAKHQFPHFLEENKI) corresponding to amino acids 1050-1064 were used. A monoclonal anti-Sall4 antibody was generated using *Sall4* cDNA encoding amino acids 95-216. The following additional antibodies were used for staining blastocysts and ES cells: monoclonal anti-Oct3/4 (Santa Cruz), rabbit antisera against Oct3/4 (Niwa et al., 2005) and monoclonal anti-Cdx2 (BioGenex). GFP-fused *Sall4* and *Sall1* zinc-finger mutants in which the cysteine residues were replaced by glycine were produced using PCR. NIH 3T3 cells were plated onto six-well plates at a density of 1×10^5 cells per well 1 day prior to transfection. The cells were transfected with 3 μg of the plasmids using FuGENE 6 (Roche) and cultured for 48 hours prior to analysis by confocal microscopy. Construction of *Sall1-GFP* and *Sall1*$^{1\text{-}435}$*-DsRed*, immunoprecipitation, immunocytochemistry and confocal microscopy were performed as described previously (Sato et al., 2004).

RESULTS

Sall4-deficient mice die shortly after implantation

Fig. 1A,B depict the strategy used to delete all the eight zinc-finger domains of *Sall4*. As *Sall4*-null mice did not survive beyond embryonic day (E) 6.5 (Table 1), the embryos were examined at E5.5-6.5 (Fig. 1C,D). Although wild-type embryos developed an egg cylinder with a central proaminiotic cavity, seven out of the 26 embryos (26.9%) derived from the heterozygous intercross barely retained a structure that resembled the epiblast. These embryos were identified as *Sall4*-null by in situ hybridization, while *Sall4* expression was observed in the epiblast, and less abundantly in visceral endoderm and extra-embryonic ectoderm in the wild-type embryos (Fig. 1D). Though the areas occupied by the epiblast markers (*Oct3/4*, *Fgf4* and *Nodal*), the trophectoderm and extra-embryonic ectoderm marker (*H19*), and the extra-embryonic ectoderm marker (*Bmp4*) were significantly reduced, they were still present in *Sall4*-null embryos (Fig. 1D and data not shown). These data demonstrate that *Sall4* is essential for embryonic development during the peri-implantation period, but not for commitment to the epiblast or extra-embryonic lineages.

Sall4 is required for inner cell mass proliferation in blastocysts in vitro

As the drastic impairment of *Sall4*$^{-/-}$ embryos hindered further examination, blastocysts from *Sall4*$^{+/-}$ intercrosses (E3.5) were examined. At this stage, the Sall4 protein was expressed both in the inner cell mass (ICM) and trophectoderm in the wild-type (Fig. 2A). Homozygotes were, however, indistinguishable from wild-type or heterozygotes, and expression of *Oct3/4* (ICM marker) and *Cdx2* (trophectoderm marker) was not altered (Fig. 2A), indicating that lineage commitment between these two lineages occurs normally. Next, cultured blastocysts were investigated for phenotypic changes. The embryos hatched from their zonae and attached to the plates, and the trophectoderm grew in an identical manner. By day 5 in culture, all homozygotes (n=14) showed significantly reduced outgrowth of ICM compared with wild-type and heterozygote (n=43) (Fig. 2B). At day 3 of culture, when the phenotype was becoming apparent, *Sall4*-deficinet ICM was positive for Oct3/4, as determined by immunostaining (Fig. 2B), and expression of the lineage markers examined by RT-PCR was not impaired: *Oct3/4* (ICM), *Gata6* and *Gata4* (primitive endoderm), eomesodermin and *H19* (trophectoderm) (Fig. 2C). These results suggest that lineage commitment does occur in the absence of Sall4. By contrast, at day 3 of culture, BrdU incorporation was significantly reduced in *Sall4*-deficient ICM when compared with wild type or heterozygote, while an apparent increase in apoptosis, as determined by TUNEL assay, was not detectable (Fig. 2D; data not shown), indicating that *Sall4* is required for ICM proliferation. Next, the trophectoderm was removed by immunosurgery to rule out secondary effects of trophectoderm abnormality. Of 54 ICMs, 41 (76%) grew into a spheroid structure with a primitive endoderm surrounding it, and all

Table 1. Genotyping of heterozygous crosses

Stage	+/+	+/–	–/–	n.d.	Total
E3.5	10	16	8	2	36
E6.5-7.5	7	16	0	5	28
E8.5-10.5	5	10	0	9	24
E11.5-13.5	10	14	0	3	27
E14.5-15.5	10	12	0	4	26
P0	80	86	0	0	166

n.d., not determined. Only implantation sites were detected.

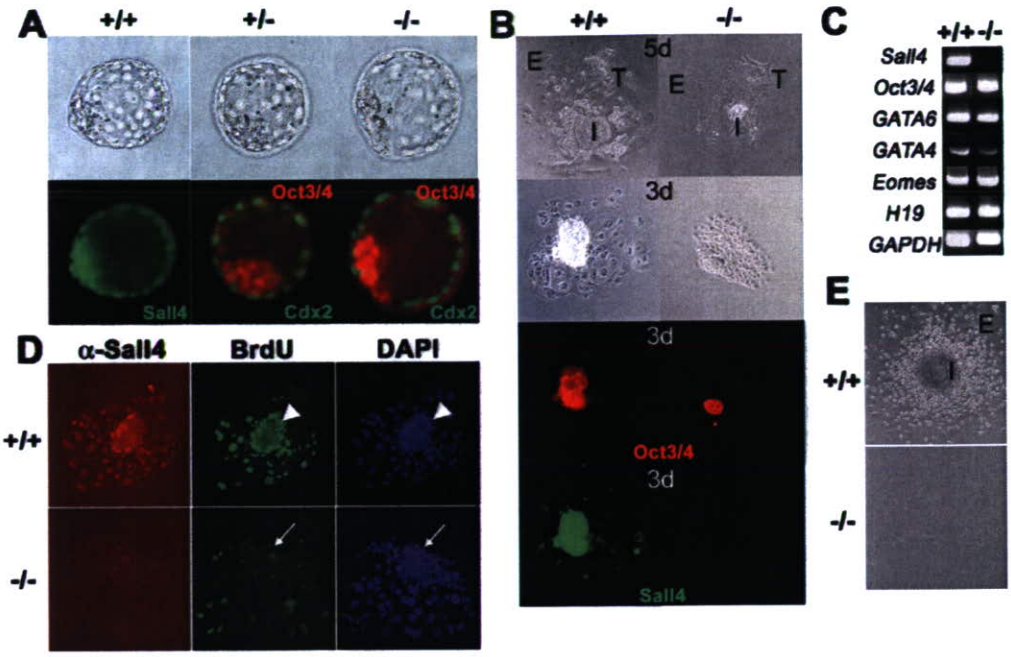

Fig. 2. Requirement of *Sall4* for inner cell mass proliferation in blastocysts in vitro. (**A**) Normal development of wild-type (+/+), heterozygous (+/–) and *Sall4*-null (–/–) blastocysts (E 3.5). Sall4 is expressed in the inner cell mass and trophectoderm (left column). Oct3/4 (red) and Cdx2 (green) staining shows that commitment to the inner cell mass and trophectoderm occurs normally in the *Sall4* homozygotes (compare middle and right columns). (**B**) Reduction of inner cell mass in *Sall4*-null blastocysts cultured in vitro. Uppermost row shows phase-contrast photo at 5 day of culture. Second row shows phase contrast at 3 day of culture. Lower two rows show immunostaining of Oct3/4 and Sall4. E, primitive endoderm; I, inner cell mass; T, trophectoderm. (**C**) RT-PCR analysis of markers in blastocysts cultured for 3 days. All the lineage markers are expressed. (**D**) Reduced proliferation of the inner cell mass of *Sall4*-null blastocysts cultured for 3 days. BrdU incorporation of the inner cell mass is reduced in *Sall4*-null blastocysts (arrow), compared with wild type (arrowhead). (**E**) Failure of growth of *Sall4*-null inner cell mass free from the trophectoderm.

the ICMs were genotyped as wild-type or heterozygote. By contrast, 13 out of 54 (24%) ICMs showed very few signs of growth (Fig. 2C rightmost column), suggesting that, independent of trophectoderm, *Sall4* is essential for ICM outgrowth.

Sall4-null ES cells show reduced proliferation

The above data prompted us to investigate Sall4 functions in ES cells, as these cells are derived from the ICM. To obtain *Sall4*-null ES cells, a vector containing the hygromycin resistance gene (*Hyg*) was introduced into heterozygous cells containing the *Neo*^{r} allele (see Fig. S1 in the supplementary material). We also attempted the reverse order, and both experiments resulted in a relatively frequent isolation of heterozygous cells in which the initial targeted allele was retargeted by the second vector. However, *Sall4*-null ES cells were isolated at a very low frequency (Table 2). To confirm these results, we constructed other versions of the vectors that contained promoterless *β-geo* or *Hyg*, thus facilitating the isolation of homologous recombinants (see Fig. S1 in the supplementary material). However, when introduced into heterozygous cells, most homologous recombinants showed retargeting of the mutated allele, and *Sall4*-null cells were obtained at a low frequency (Table 2). Therefore, the absence of *Sall4* is disadvantageous to ES cells.

We next tried inducible knockdown of *Sall4* by introducing siRNA oligonucleotides into ES cells. siRNA against *Sall4* efficiently reduced *Sall4* expression by day 2 after transfection, but *Sall4* expression recovered by day 4 (Fig. 3A), which was also confirmed by Sall4 immunostaining on ES colonies (data not shown). *Sall4*-siRNA-treated cells showed transient reduced growth with similar kinetics to the *Sall4* expression, while negative control siRNA had no effect (Fig. 3B). By contrast, colony morphology and Oct3/4 staining were not altered in the absence of Sall4 (data not shown). These data suggest that *Sall4* may be required for proliferation of ES cells.

Next, heterozygous cells were generated containing a floxed allele of *Sall4* by homologous recombination (see Fig. S1 in the supplementary material). When the *Sall4-IRES-Hyg* vector was introduced into this clone, both alleles were targeted with a similar frequency (wild-type allele, 10/23; floxed allele, 11/23), resulting in two types of cells: flox/– and +/– (Fig. 3C). As shown by western blot, *Neo*^{r} in intron 2 of the floxed allele did not affect Sall4 expression, and there was no difference in proliferation between the two types of cells. Upon infection with adenovirus expressing Cre, flox/– cells became almost *Sall4*-null by day 3, while +/– cells served as a negative control, as determined by western blot (Fig. 3C). Indeed, when cells were subsequently replated and single clones

Table 2. Generation of *Sall4*-null ES cells

Experiment	Vectors		Selection at second round	Number of colonies	Integration event		
	First round	Second round			Random	Retargeting	Second allele
1	*pGK Neo*	*pGK Hyg*	Hyg	134	116	16	2
2	*pGK Hyg*	*pGK Neo*	Neo	115	68	44	3*
3	*IRES Hyg*	*IRES β-geo*	Neo	20	12	8	0
	IRES Hyg	*IRES β-geo*	Neo+Hyg	13	12	0	1*

Two rounds of targeting were carried out to disrupt both the alleles of *Sall4* in ES cells.
*Two out of three clones in Experiment 2 and one clone in Experiment 3 were finally dominated by contaminating heterozygous cells.